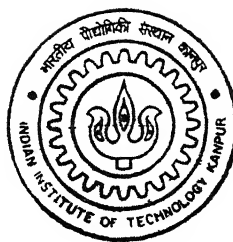


ent

9910548

THERMO-EMF ANALYSIS OF FLANK WEAR IN TURNING

by
VIVEK. M. MUTTUR



TH
ME/2001/M
M985t

DEPARTMENT OF MECHANICAL ENGINEERING
INDIAN INSTITUTE OF TECHNOLOGY, KANPUR

February, 2001

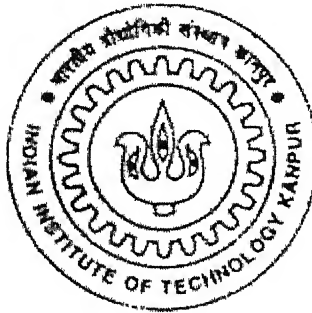
THERMO- EMF ANALYSIS OF FLANK WEAR IN TURNING

A thesis submitted in partial fulfillment of the
Requirements of the degree of

MASTER OF TECHNOLOGY

BY

VIVEK. M. MUTTUR (9910548)



DEPARTMENT OF MECHANICAL ENGINEERING

INDIAN INSTITUTE OF TECHNOLOGY KANPUR

FEBRUARY 2001

5 FEB 2003 / ME

पुस्तकालय, व.पी.नाथ केलकर पुस्तकालय
भारतीय प्रौद्योगिकी संस्थान कानपुर


अवधि क्र० A 141974



A141974

CERTIFICATE

This is to certify that the work under the thesis titled **Thermo-Emf Analysis of Flank wear in turning** by **Vivek. M. Muttur (Roll No. 9910548)** has been carried out under my supervision and this work has not been submitted elsewhere for a degree.



Dr. S. K. Choudhury

Professor.

Department of Mechanical Engineering.

IIT Kanpur.

ACKNOWLEDGEMENTS

I would like to express my gratitude to my thesis supervisor Dr. S. K. Choudhury for his skillful guidance, constant supervision and suggestions, which helped me in completing my thesis.

I would wish to thank Mr. R. M. Jha, Mr. H. P. Sharma and Mr. Namdeo for their help during the experimental work. Their experience and expertise helped me to solve many of the practical problems encountered.

Finally, I thank all my friends, who made my stay in this institute a memorable and an enriching experience.

CONTENTS

List of figures.....

List of Tables.....

Abstract.....

1. CHAPTER 1

1.1 Introduction..... 1

1.2 Literature Survey..... 2

1.3 Organisation of the Thesis..... 9

2. CHAPTER 2

2.1 Theoretical Analysis.....11

2.2 Wear Mechanisms and Types of wear.....14

2.3 Diffusion wear..... 16

2.4 Relation between the flank temperature and the flank wear land.....17

3. CHAPTER 3

3.1 Design of Experiments..... 20

3.2 Experimental Procedure.....24

3.3 Calibration Procedure.....26

4. CHAPTER 4

4.1 Results of Calibration.....27

4.2 Regression Equation and its validity.....27

4.3 Effect of various parameters on the temperature and flank wear
land.....32

4.4 Effect of various input parameters on temperature and flank wear (WC vs
EN24)..... 33

5. CHAPTER 5

5.1 Conclusions.....58

5.2 Scope for future work.....58

REFERENCES

List of Figures

2.1 Sources of heat generation in metal cutting.....	11
2.2 Friction existing at the chip tool interface.....	13
2.3 Change in flank wear land with time	16
3.1 Experimental set up used for temperature measurement.....	25
4.1a Calibration curve for HSS vs EN24 Steel.....	39
4.1b Calibration curve for WC vs EN24 Steel.....	39
4.2 Variation of temperature vs speed at 0.1mm/rev feed.....	40
4.3 Variation of temperature vs speed at 0.15mm/rev feed.....	40
4.4 Variation of temperature vs speed at 0.2mm/rev feed.....	41
4.5 Variation of temperature vs depth of cut at 32 RPM.....	41
4.6 Variation of temperature vs depth of cut at 80 RPM.....	42
4.7 Variation of temperature vs depth of cut at 125 RPM.....	42
4.8 Variation of temperature vs feed at 32 RPM.....	43
4.9 Variation of temperature vs feed at 80 RPM.....	43
4.10 Variation of temperature vs feed at 125 RPM.....	44
4.12a Variation of flank temperature vs flank wear at 32 RPM and 0.1mm/rev feed.....	45
4.12b Variation of flank temperature vs flank wear at 32 RPM and 0.15mm/rev feed.....	45
4.12c Variation of flank temperature vs flank wear at 32 RPM and 0.2mm/rev feed.....	46
4.13a Variation of flank temperature vs flank wear at 80 RPM and 0.1mm/rev feed.....	46

4.13b Variation of flank temperature vs flank wear at 80 RPM and 0.15mm/rev feed.....	47
4.13c Variation of flank temperature vs flank wear at 80 RPM and 0.2mm/rev feed.....	47
4.14a Variation of flank temperature vs flank wear at 125 RPM and 0.1mm/rev feed.....	48
4.14b Variation of flank temperature vs flank wear at 125 RPM and 0.15mm/rev feed.....	48
4.14c Variation of flank temperature vs flank wear at 125 RPM and 0.2mm/rev feed.....	49
4.15 Variation of temperature with depth of cut at 125 RPM.....	50
4.16 Variation of temperature with depth of cut at 160 RPM.....	50
4.17 Variation of temperature with depth of cut at 200 RPM.....	51
4.18 Variation of temperature with Rotational speed at 0.2mm/rev Feed.....	51
4.19 Variation of temperature with Rotational speed at 0.25mm/rev Feed.....	52
4.20 Variation of temperature with Rotational speed at 0.3mm/rev Feed	52
4.21 Variation of temperature with feed at 125 RPM.....	53
4.22 Variation of temperature with feed at 160 RPM.....	53
4.23 Variation of temperature with feed at 200 RPM.....	54
4.24 Variation of flank wear with flank temperature at 125 RPM.....	55
4.25 Variation of flank wear with flank temperature at 160 RPM.....	55
4.26 Variation of flank wear with flank temperature at 200 RPM.....	56
4.27 Variation of flank wear with flank temperature at 1mm depth of cut...	56

4.28 Variation of flank wear with flank temperature at 1.5mm depth of Cut.....	57
4.29 Variation of flank wear with flank temperature at 2.0mm depth of Cut.....	57

List of Tables

- 3.1. The factors set according to the 3^3 factorial design (HSS vs EN 24 Steel) (22)
- 3.2 The factors set according to the 3^3 factorial design (WC vs EN 24 Steel).....(23)
- 4.1 Input Parameters and corresponding temperature and flank wear ...(29)
- 4.2 Theoretical and Experimental values of temperature(30)
- 4.3 Theoretical and Experimental Flank wear h_f (31)
- 4.4 Input Parameters and corresponding temperature and flank wear (WC vs EN 24 Steel).....(34)
- 4.5 Theoretical and Experimental Temperatures for WC vs EN 24 Steel.....(35)
- 4.6 Theoretical and Experimental Flank wear h_f for WC vs EN 24 Steel..... (36)

Abstract

Tool wear is a dominant phenomenon that affects the tool life. Flank wear is the common type of wear, which leads to tool failure. In the present work, flank wear has been monitored indirectly by measuring the temperature generated during the machining process. Temperature is one of the most important variables measurable during the machining process. Experiments have been carried out using HSS tool and tungsten Carbide tool bits. The three input parameters used in the experiments are rotational speed (rpm), feed (mm/rev) and depth of cut (mm). Empirical relation between the temperature θ and the input parameters as well as between the flank wear land and the input parameters have been established for both the set of experiments. Experimental values of temperature and flank wear land have been compared with the theoretical values. Temperature generated at the flank θ_f has been assumed to be approximately 4% of the total temperature θ and this is related to the flank wear land.

CHAPTER 1

1.1 Introduction

Cutting tools are subjected to a several rubbing process as the chip slides on its rake face and when the flank face rubs against the machined work piece surface. Machining of high strength metals and alloys is limited by the tool life and ways must be found to increase it. Tool life is predominantly affected by tool wear.

Crater wear and flank wear are the two types of wear, which are identified during the machining process. The measure of flank wear is given by a single dimension, h_f , the flank land width. The crater wear is defined by the volume of material removed from the rake face in the form of crater. The flank wear is the commonly used measure for predicting the failure of the cutting tool.

The on-line tool wear monitoring has been a subject of research for many years. Due to the advent of adaptive control and Computer Integrated Manufacturing (CIM), there has been a spurt in research in this field of manufacturing. Advances in adaptive control and CAM call for sensitive ways of measuring tool wear. No single universal method of tool wear monitoring has been developed which is suitable for all applications.

A number of methods of tool wear and failure sensing techniques have been developed over the years, but very few have been used in industries successfully. It has been shown that tool failure contributes, on an average, upto 6.8% to the downtime of the machining centers [1].

Tools fail either by fracture or by gradual wear. Mostly the tools made of brittle materials fail by fracture. In case of the gradual wear, the tool reaches the limit of its life by either flank wear or crater wear. Flank wear and crater wear failures have formed the subject of most studies in the area of tool wear. More methods have been developed for tool wear sensing than models that correlate tool life with parameters describing the machining environment [2]

Broadly the tool wear sensing techniques can be classified into two major categories

- 1) Direct, where the actual tool wear is measured.

2) Indirect, where a parameter correlated with tool wear is measured.

In indirect measurements, various parameters which vary along with the tool wear are measured and these are correlated with the wear occurring on the tool.

The different parameters which can be measured are: cutting force, acoustic emission from the tool surface, sound, vibration, temperature, power input, roughness of the machined surface etc.

1.2 Literature Survey:

Cutting force is one of the parameters of machining that can be easily measured. Cutting force changes as the tool wears and is often used as a method to detect tool wear in the laboratory. Some experimental results show [3] that there exists a linear relationship between the feed and the thrust forces and the tool wear. Some authors [3] have claimed that it is impossible to derive accurate information on tool wear based on measurements of cutting forces in turning. This is because significant increase in forces occurs only at the moment of tool failure. Thus only tool failure can be detected and not tool wear and its various forms.

Acoustic Emission (AE) has also been used as a means of sensing tool wear or tool fracture. The spectra of the AE signals is used to detect the tool wear and tool failure. The method is based on pattern recognition concepts. Flank wear of a cutting tool was successfully measured by monitoring the gradual increase of the AE signal [4]. AE spectral analysis is considered to be a poor method for single point tools where marked periodicity was absent. A disadvantage of this method is the combined effect of flank and crater wear, making it difficult to exactly determine the wear conditions of the cutting tool through AE analysis. Another potential source of error is the influence of the cutting parameters on the AE response. This might mask the information coming from the wear conditions. Sound from the machining zone has been used to monitor the conditions of the cutting edge. This method is impractical to be employed in a shop floor environment due to the high level of the ambient noise [5].

Vibration occurs as the work piece and the chips rub against the worn tool and this information can be used in various ways to detect the tool wear and tool fracture.

Ultrasonic signals in their normalized form have been used by some researchers to detect in-process gradual wear during turning operations [6]. The experiments were conducted and it was shown that gradual wear can be made tool independent by normalizing the measurements with the calibration mark. This method was only useful for turning operations and with inserts which have a negative rake angle.

The roughness of the surface on the work piece machined is influenced by the sharpness of the tool. This is used for tool condition monitoring. A fibre optics transducer was used for in-process indication of surface roughness during a finish turning process [7].

Cutting temperature increases during the machining process and this has an effect on the tool life. Hence cutting temperature can be used to monitor tool failure. Several techniques have been reported for assessing cutting temperatures [8]. The most commonly used techniques are the work- tool thermocouples and the tool thermocouples. Reference [9] gives a review of the methods that are used for measuring the machining temperatures.

Zakaria and Gomayel [10] explored the reliability of cutting temperature for monitoring tool wear. Long duration turning tests employing different speed, feed and depth of cut were conducted. The cutting temperature was sensed on-line using the tool-work piece thermocouple technique. From the experimental results it was found that the thermal voltage signal was the parameter which was very sensitive to the cutting conditions. They were of the opinion that cutting temperature as measured by the work-tool thermocouple cannot be used by itself to predict the status of the wear on the cutting tool.

P. Mathew [11] used the predicted cutting temperature in determining the tool performance. Dynamic flow stress and temperature properties of the work material were used to determine tool performance when machining plain carbon steels. It was shown that there is a relationship between the tool wear in

logarithmic scale and the reciprocal of the absolute temperatures achieved at the chip-tool interface. This indicated the presence of the temperature dependent wear mechanism. It was shown that a diffusion-based equation could be used to effectively relate the wear rate of a carbide tool to the temperature of the tool when considering the turning process. At high tool temperatures diffusion was found to be the basic mechanism involved in wear.

Groover, Karpovich and Levy [12] studied the relationship between remote thermocouple temperatures and the tool wear in machining. They demonstrated that a strong correlation existed between the tool wear and the signal of a thermocouple at a position on the cutting tool remote from the cutting edge. They proposed a mathematical model to explain the relationship between tool wear and temperature. As the tool wear progresses on the cutting tool, they found that the net effect is to increase the amount of energy flowing into the tool at the cutting edge. A linear relation between the tool wear and temperature measured by the remote thermocouple was proposed which also incorporated a term for converting temperature difference into a wear difference above the initial value. The model provided a high degree of agreement between the actual and the estimated tool wear.

The effect of tool flank wear on the tool chip interface temperature was studied by Olberts [13]. Tool –work thermocouple technique was used to measure the interface temperature. In the experiment the effect of ground-on wear land on interface temperature was studied. Wear lands were ground on the tools to eliminate crater wear as a variable. It was found that the tool-work interface temperature was considerably lower than the tool-chip interface temperature as the wear land forms. The tool-wear interface temperatures then increase continuously as the wear land increases. The chip thickness ratio gave an indication of the degree of tool wear for wear lands up to 0.02inch and more the land wear, the lower the chip-thickness ratio.

Levy, Tsai and Groover [14] studied the effect of crater wear on the response of a remote thermocouple sensor. This technique depends for its operation on the strong influence of the wear on the transient temperature

variations in the tool. Results were obtained under idealized cutting conditions with a zero wear rate, a normal wear rate and an accelerated wear rate. The three cases were then compared to study the effect of wear on temperature. A transient finite difference analysis for the temperature variations in a tool and chip was presented. The results indicated that the temperatures at the base of the tool insert are quite sensitive to tool wear with increase in temperature due to the growth of the wear crater which are of the order of 30.6k/mm.

Lenz, Katz and Ber [15] investigated the flank wear of cemented carbide tools. They found that heat generated during cutting in several zones leads to an assortment of elevated temperatures. These temperatures vary when tool material properties are changed. Different levels of temperatures were found to have an influence on the tool life. A set of tests employed an electrical analogue, which was accompanied by basic heat transfer calculation. This supplied information on the magnitude and distribution in the flank zone. The results of the electrical analogue test helped to calculate the temperatures in the tool-work interface. The significance of the flank wear size and its dependency on rake face occurrence may be deduced from these temperature magnitude. They concluded from these tests, that heat generated is higher for TiC tools relative to those of WC tools. Due to the effect of the thermal properties of the tool material, a certain temperature will be generated at the flank and its vicinity. This causes a thermal wear mechanism to take place and hence defining the tool life.

Constriction resistance concept was applied to wear measurement of cutting tools by Wilkinson [16]. A mathematical model for the tool-work piece interface resistance in a single point oblique cutting operation was described. The model was developed using the concept of constriction resistance. It was shown that the resistance measurements might be used to calculate the amount of wear on the cutting tool as the cutting proceeds. This method gives the mean value of the flank-wear land width. It was found that there was a good measure of agreement between the in process and optical measurements. Resistance of the tool-workpiece interface in metal cutting was concluded to be a very

important parameter which may be used to measure the tool wear during the process.

Leshock and Shin [17] investigated the effect of tool face temperature (measured by thermocouple) on the tool flank and crater wear mechanisms. Steel alloys were used as the workpiece material. Experimentally they determined the flank wear at lower speeds (1.29-2.49 m/s) so that crater wear does not affect the measured temperatures. After a fairly high value of flank wear was attained, they found that the tool would fail and tool temperatures could no longer be measured.

Crater wear measurement was performed using the laser triangulation technique, with the equipment consisting of a laser sensor and a co-ordinate measuring machine (CMM). This is due to the fact that crater wear is measured in terms of volume or depth. The volume wear was compared with the measured temperature. The results showed that crater volume wear rate is a quadratic function of temperature. This is because crater wear is a diffusion-based phenomenon dependent on temperature.

Chow and Wright [18] measured on-line temperature in a turning operation. The measuring scheme relied on the signal from a standard thermocouple. The unique feature was that the scheme predicted the interface temperatures for an interrupted cut and also when there is tool wear. They found that cutting temperature can be considered as an ideal control variable purposes because of its correlation with tool wear.

Takeyama and Murata [19] found a relation between the flank wear and the cutting temperature. They found that the flank wear first increases slightly with cutting edge temperature but after a critical value (about 1200 K) it starts to accelerate. This is because at high temperatures both flank and crater wear are dominated by diffusion. Thus they opined that due to correlations existing between the interface temperatures and wear mechanisms, a control over the wear process is possible. This control can be exercised if cutting edge temperature and maximum temperature at the rake face can be monitored during the process.

Smart and Trent [20] measured the temperature gradients in high-speed steel tools used for machining of iron, titanium and nickel. The gradients wear measured based on the structural changes in HSS heated to temperatures over 560° C. These three metals imposed their own and greatly different pattern of temperature within the tool. It was shown that this controls some of the basic wear processes which limit the rates of metal removal. The results by these experiments have relevance to the understanding of tool wear, the design of cutting tools and the application of cutting lubricants. They drew the conclusion that temperature distribution and the influence of speed and feed must be dependent on factors such as clearance and rake angles. Their work emphasized the overriding importance which temperature distribution can have on the performance of the cutting tools.

Aay and Yang [21] made an experimental study to monitor timewise temperature variations of the tool and workpiece in orthogonal cutting. They used both thermocouples and infrared thermovision. They found that the progress of wear is accompanied by a consistent increase in temperature of the tool which in turn accelerates the wearing process. They identified two kinds of wear from a plot of the steady state temperature. They are the mechanical wear in the lower cutting speed zone and diffusion wear in the higher cutting speed zone. A critical value for transition from mechanical wear to diffusion wear has been identified. The rate of decrease in tool life is faster in the mechanical wear zone and slower in the diffusion zone.

Wu and Meyer [22] proposed an empirical general cutting tool temperature predicting equation in terms of speed, feed and depth of cut. The equation was based on response surface methodology. A second order model was proposed based on least square estimation. They found the importance of feed and depth of cut on temperature response. The second order cutting tool temperature equation is necessary to yield a more accurate prediction at high temperature range.

Venuvinod, Lau and Rubenstein [23] have shown that the assumption of continuous contact at the tool work interface in metal cutting, leads to results

which are in conflict with empirical evidence. They proposed a new model based on discrete contact at the tool flank and the associated thermal constriction resistances were developed. A representative value of the flank temperature can be calculated from the proposed model for different cutting conditions. A relation between the flank temperature and flank wear was developed using the same discrete flank contact idealization. They developed a new parameter θ_{fs} at the tool flank land area which reflects the discrete nature of tool work contact. The discrete contact assumption was observed to overcome all the anomalies of the continuous tool work contact assumption.

Braiden [24] investigated the limits of accuracy imposed on the tool workpiece thermocouple technique by the need for an exact calibration curve for the materials being investigated. The overall accuracy of the temperature measurement depends on the accuracy achieved in finding this thermoelectric relationship. The results obtained from the calibration showed that calibration curves of WC were of parabolic nature.

Boothroyd, Eagle and Chisholm [25] made investigations of the temperature generated on the work flank of a cutting tool. They found that approximately 60% of the heat generated in the cutting region is conducted into the work piece, the remainder being removed by the chip. They opined that in majority of practical cutting operations, the life of the cutting tool is limited by the rate of wear on its flank, wear on the rake face being of secondary importance. They argued that the tool work thermocouple gives only an average temperature in the cutting zone and cannot be independently employed to measure the flank wear land. They found that though there is information about the temperature prevailing on the rake face of the tool, very little knowledge is available about the temperature conditions at the flank face of the tool. WC tools with an artificial (initial) wear land of 0.015 to 0.045(mm) were used in the experiments. They found that an increase in flank wear land leads to both an increase in the mean flank temperature as well as the mean temperature over the face and the flank. Thus the signal from the work tool thermocouple could be argued to bear some relation to the wear on the flank.

S.M. Wu [26], studied the tool life response by an analytical method. He proposed a first order relation between the input parameters and the tool life. Least square regression analysis was used to derive the analytical relationship. In the second paper [26a] he proposed a second order relation that included the interaction between the input parameters. The second order relationship was more general as compared to the first order relationship and there was a good agreement between the experimental and the theoretical results.

Gerry Byrne [27] studied the various temperature responses for different work materials when machined by HSS cutting tools. Although the temperature for different materials was different there was a general trend which showed that the temperature increased parabolically with the cutting speed. Furthermore the variation of temperature with the feed was of a similar nature. The temperature increased almost linearly with the increase in depth of cut.

In the present work the temperature during the cutting process is expressed in terms of the flank temperature and the effect of this temperature on the flank wear of the cutting tool is explored for different cutting parameters which are decided according to the design of experiments. Factorial design has been used to fix the cutting parameters.

ORGANISATION OF THE THESIS:

Chapter 1 gives an introduction about the tool wear and a brief review of the literature of the research in this area with particular reference to the thermally activated wear mechanisms.

Chapter 2 deals with the theoretical aspects of the temperature phenomena in metal cutting and details of the relations between the flank wear and the flank temperature.

Chapter 3 gives details about the factorial design which has been used for conducting the experiments. The experimental procedure as well as the calibration procedure have been explained.

Chapter 4 includes the details of the experimental results.

Chapter 5 includes the conclusion and the scope for future work.

Chapter 2

Theoretical Analysis

Introduction:

The temperature that arises in a machining operation is fundamental to the process of chip removal. It is perhaps the single most important factor influencing the efficiency of the process. The characteristic factors, which are influenced by temperature, are:

- a) The degree of plastic deformation.
- b) Extent of tool wear
- c) Degree of diffusion and corrosion

The high temperature has a very strong influence on the tool wear rate through the mechanisms of increased adhesion, diffusion and abrasion. Several techniques have been developed to evaluate the temperatures arising in the cutting zone.

Heat generation during metal cutting occurs in three distinct regions. They are:

- a) The shear zone, where heat is generated due to plastic deformation of work piece material.
- b) The chip-tool interface zone where heat is generated due to frictional rubbing between the rake face of the tool and the chip.
- c) The work tool interface zone where heat is generated due to frictional rubbing between the flank face of the tool and the work piece.

The portion of heat that flows into the tool causes very high temperatures in the vicinity of the tool tip which in turn decreases the hardness of the of the tool. The wear rate of the tool, therefore, increases resulting in a decrease in the useful life of the tool. The thermal stresses developed due to high temperature also contribute to the failure of the tool.

Cutting speed is the most important variable affecting the cutting temperature, while feed is the next important variable, followed by the depth of

cut. It has been shown experimentally that chip- tool interface temperature increases approximately parabolically with increase in cutting speed.

During the cutting process severe plastic deformation takes place in the primary and secondary zones and rubbing on rake and flank faces. The work done in effecting plastic deformation reappears in the form of heat. The flow of chip along the tool rake face is another source of heat generation. Similarly, the rubbing of the machined surface on the flank face due to elastic recovery and wear of flank face, is yet another source of heat generation. These sources of heat generation are shown in Fig. 2.1.

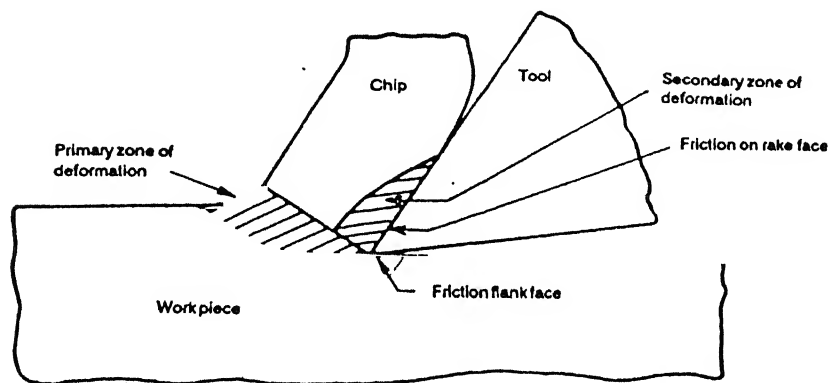


Fig 2.1 Sources of heat Generation in metal cutting (From Juneja and Sekhon).

Maximum heat is developed in the material, which forms the chip, and hence it is the hottest portion of metal in the cutting process. Some heat from the machining zone gets conducted into the work piece and into the tool through the chip-tool interface. The rise of temperature of temperature in the tool and work piece gives rise to early wear of the tool and dimensional inaccuracy of the machined surface.

2.1 Theoretical Analysis:

The shear plane temperature rise can be approximately estimated by assuming the thin zone model of metal cutting and by assuming that there is a uniform rise of temperature all over the shear plane.

If E_s is the energy per unit volume dissipated at the shear plane, then

$$\theta_s = \lambda E_s / J\rho_w C_w + \theta_i \quad (2.1)$$

Where, θ_s is the temperature at the shear plane;

θ_i is the initial temperature of the work material;

E_s is the energy/ unit volume dissipated at the shear plane;

J is the heat equivalent of mechanical energy;

ρ_w is the density of work material;

C_w is the specific heat of the work material;

λ is a factor representing the fraction of heat retained in the chip;

E_s is given by

$$F_s V_s / btV \quad (2.2)$$

Where, F_s = force on the shear plane

V_s = velocity of the tool along the shear plane

b = width of the chip

t = thickness of the chip

V = velocity of the chip

In the secondary deformation zone (along the rake face), heat generation is caused by the plastic deformation of the chip (which is negligible since the rate of deformation is not very high), sliding and large frictional forces between the tool and the chip. Wallace and Boothroyd [28] concluded that the normal stress, p , increased exponentially towards the cutting edge as shown in Fig. 2.2

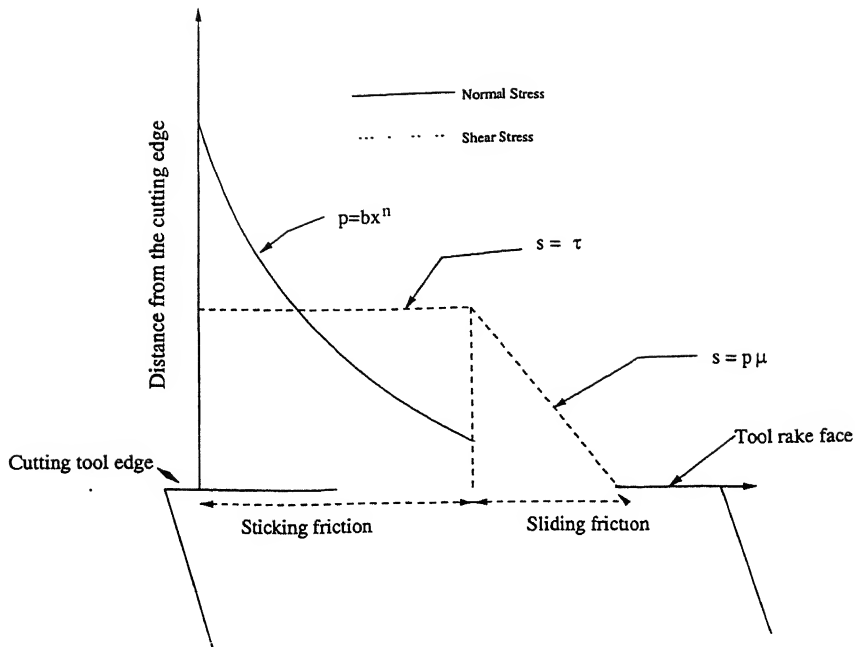


Fig.2.2 Friction existing at the chip tool interface

In the secondary zone, heat is generated over the contact length due to boundary friction. The heat generation rate per unit area q_x due to boundary friction at a point on the contact length at a distance x from the tool edge was calculated as

$$q_x = \tau_x V_x \quad (2.3)$$

Where V_x is the chip velocity at a distance x from the tool edge.

The heat is generated on the flank face of the tool due to boundary friction. It is assumed that the distribution of the shear stress on the flank face of the tool is uniform ie,

$$\tau_f = F_f / b l_f \quad (2.4)$$

Where F_f is the force component due to boundary friction parallel to the flank measured experimentally, b is the width of cut and l_f is the length of flank wear land measured along the flank face.

The rate of heat generation per unit area over the length of flank wear due to boundary friction is estimated as

$$q_f = \tau_f V_f \quad (2.5)$$

where, V_f is the velocity along the flank face.

During the cutting operation, the tool is subjected to cutting forces that are concentrated over a relatively small contact area on the rake and the flank. The temperatures over the contact surfaces are very high. The tool is subjected to mechanical and thermal shock during the entry and exit of a cut. Under such severe conditions, tools gradually wear out.

2.2 Wear Mechanisms and Types of wear

There are different wear mechanisms by which a tool wears.

- a) Shearing at high temperatures: The tool wears due to thermal softening.
- b) Diffusion wear: Due to high temperature existing at the interface, atoms of the harder material diffuse into the softer matrix, thereby increasing the latter's hardness. This is strongly dependent on temperature.
- c) Adhesion wear (Attrition wear)
- d) Abrasive wear.

The wear of the tool occurring on the rake face (crater wear) and/or on the flank face (flank wear) are of the following nature.

Flank wear: Wear lands are produced on the side and end flanks of the tool on account of the rubbing action of the machined surface. This wear land develops and grows on account of abrasion and adhesion. The wear land is not of uniform width. The frictional stress and maximum temperature at the flanks also go on increasing with time. A stage is reached when diffusion becomes the predominant wear mode on the flank. After a critical wear land has formed, further wear takes place at an accelerating rate. During the steady wear phase (which is the useful life of the tool), flank wear is mainly caused by abrasion, whereas during the rapid wear phase, it is caused by diffusion.

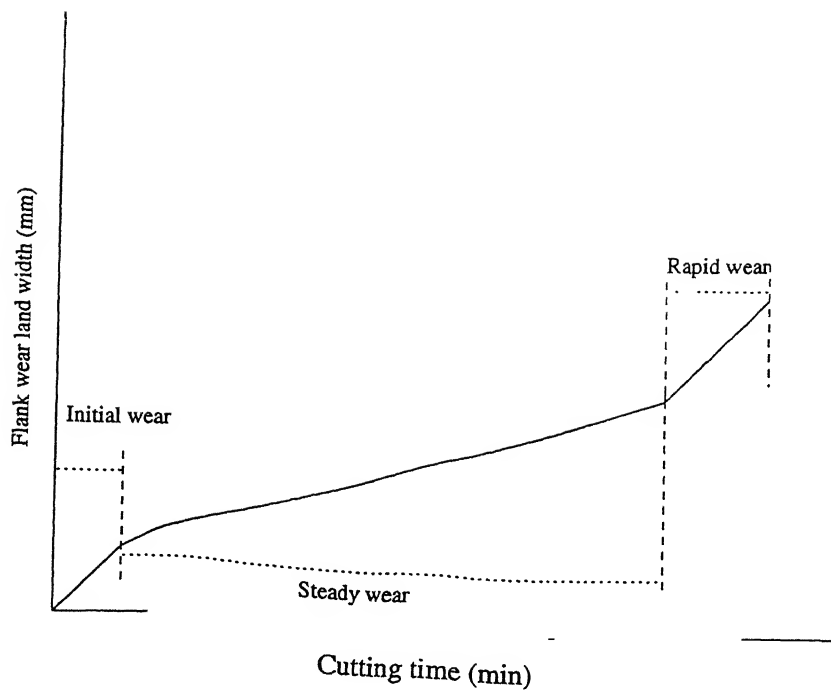


Fig.2.3 Change in flank wear land with time

Flank wear is easily measured with the help of a microscope because it is given by a single dimension namely the wear land width, h_f .

Crater Wear: It occurs in the form of pit on the rake face. The crater is formed at some distance from the cutting tip. The location of the maximum cratering and maximum chip tool interface temperatures coincide with each other. Hence it may be assumed that cratering is a temperature dependent phenomenon caused basically by diffusion. The crater significantly reduces the strength of the tool and may lead to total failure of the tool.

Under normal cutting conditions, flank wear develops much faster than crater wear. As such tools tend to fail due to flank wear long before crater wear becomes significant. Therefore flank wear is the more common measure of tool life under normal cutting conditions [29].

Cutting tool wears have long been recognized as temperature activated mechanisms. Thus it would be desirable to make temperature measurements during machining to correlate the same with tool wear. The only laboratory method, which appears promising temperature measurements is, the tool-work thermocouple method [30].

The tool-work thermocouple method measures the average interfacial emf. This emf corresponds directly to the average interfacial temperature under two conditions: (i) When the interfacial temperature is uniform, and (ii)

when the temperature and the thermo-emf are related linearly [31].

The thermo-emf generated during the turning process consists of the dc Components as well as the ac components. The dc component is obtained due to the Seebeck effect, which occurs due to the movement of free electrons within the rigid lattice structure of the atoms in the conductor.

The Fermi effect is inherently a contact phenomena due to electron transfer from a conductor with a smaller work function to a conductor with a larger work function. (Work function is the minimum energy required in Mev to remove the electrons from the outermost shell of the atom). The turning process involves a continuous succession of contact forming and breaking. The contact durations may vary with the area of contact and the sliding velocity at the chip-tool interface. [31]

2.3 Diffusion wear:

Diffusion wear occurs at the chip tool interface and the flank face.

The diffusion can be analysed by the Fick's Law. It states that the rate of change of concentration dc/dt of the diffusing constituent is proportional to the mass input in the y-direction (i.e., in the direction of diffusion across the wear land at the flank). Mathematically the law is expressed by

$$dc/dt = D\partial^2 c / \partial y^2 \quad (2.6)$$

where D is the diffusion coefficient which is dependent on temperature and is given as

$$D = D_0 e^{-Q/RT} \quad (2.7)$$

where, D_0 = constant

Q = activation energy for the diffusion process

R = Universal gas constant

T = absolute temperature, assumed constant over the flank length h_f .

Solving equation (2.7), we get the flow of diffusion mass, M_f across the flank face in time τ_f as ,

$$M_f = 2C_0 h_f b \sqrt{D\tau_f / \Pi} \quad (2.8)$$

C_o = Concentration of the diffusing constituent at the interface $y = 0$.

Substituting the value of D in equation (2.8), we get, C_o

$$M_f = 2C_o h_f b \sqrt{D_o \tau_f} / \Pi e^{(-Q/2RT_f)} \quad (2.9)$$

Higher the values of the flank wear land h_f , the width of cut b , time τ and flank face temperature T , greater would be the amount of the diffused mass .

2.4 Relation between the flank temperature and the wear land:

Layer removal under plastic deformation may be considered as a reasonable assumption because of the high magnitude of the contact stresses.

The rate of wear can be expressed as [32]

$$\frac{dw}{dt} = \frac{Z}{H} [P^{3/4} V_c] \quad (2.10)$$

where H = Hardness of the tool material

Z = Wear coefficient depending on the metals in contact, nature of contact, and temperature of the contact surface

P = normal force on the surface

V_c = velocity of cutting.

Archard [33] has shown that the rate of loss of tool material depends on the nature of contact, whether elastic or plastic and also depends on normal force acting on the interface. The rate of tool material loss also depends on the sliding velocity or cutting velocity V_c .

At the flank surface, the nature of tool material removal can be considered as elastic or plastic layer removal type below a critical temperature, θ_c . When the prevailing temperature at the flank is greater than the critical temperature, θ_c , the tool material removal would be plastic lump removal type.

The flank wear rate of the tool can be written as [32]

$$dw/dt = Z_o / H V_c^{1+(m/2)} P^n \quad (2.11)$$

n = a factor depending on the type of material removal, layer or lump type.

m = factor depending on the nature of contact (either abrasion or adhesion) and also dependent on the cutting speed.

The flank wear rate is also given as [32]

$$dw/dt = Z_0 / HV_c^{1+(m/2)} P^n \quad (2.11)$$

n = a factor depending on the type of material removal, layer or lump type.

m = factor depending on the nature of contact (either abrasion or adhesion) and also dependent on the cutting speed.

The flank wear rate is also given as [32]

$$dw/dt = b\Psi h_f dh_f / dt \quad (2.12)$$

From equation (2.11) assuming that hardness H does not vary much in the temperature insensitive region we get,

$$Z_0 / V_c^{(2+m)/2} P^n = b\Psi h_f dh_f / dt \quad (2.13)$$

$$\text{or, } Z_0 V_c^{(2+m)/2} P^n dt = b\Psi h_f dh_f \quad (2.14)$$

Where b = width of cut

$\Psi = \rho \tan \alpha / (1 - \tan \gamma \tan \alpha)$, a factor dependent on the tool geometry.

ρ = density of the tool material.

γ = rake angle

α = clearance angle

Solving equation (2.14) we get

$$h_f = [(2-n)BZ_0 V_c^{(2+m)/2} / b\Psi]^{1/(2-n)} T^{1/(2-n)} \quad (2.15)$$

where T = time at which the flank wear is considered .

For the temperature insensitive region n = 3/4,

Therefore, from equation (2.15) we get

$$h_f = [5/4 Z_0 A^{3/4} B / b\Psi] V_c^{0.4(m+2)} T^{0.8} \quad (2.16)$$

At moderate cutting speeds m = 4, the equation of wear becomes

$$h_f = K^* V_c^{2.4} T^{0.8} \quad (2.17)$$

K^* = Constant dependent on the thermal properties of tool-work pair

Ghosh et. al [34] have shown that for a given temperature, θ_f , after the initial break- in wear, a relationship can be obtained as,

$$V_c h_f = K_f \theta_f^2 \quad (2.18)$$

K_f = Constant dependent on the thermal properties of the tool –work pair.

$$h_f^* = K^* [K_f \theta_f^2 / h_f^*]^{2.4} T^{*0.8} \quad (2.20)$$

Simplifying we have

$$h_f^* = K_v (\theta_f^*)^{1.41} (T^*)^{0.236} \quad (2.21)$$

$$\text{Where, } K_v = K^* (K_f^{2.4})^{1/3.4}$$

Thus the flank wear land, h_f can be related to the temperature at the flank.

In the present work the temperature measured with the tool-work thermocouple is the average temperature in the cutting zone. To relate it to the temperature at the flank, the assumption is made that about 16% of the heat generated is from the rake face of the tool and approximately 4% is generated from the flank. This is because otherwise it is very difficult practically to separate the rake and the flank temperature from the thermocouple signal. Some methods have been proposed [35] when machining with split carbide tools. Thus from the temperature signal obtained from the thermocouple, the temperature at the flank is determined. This is related to the flank wear land, h_f by the relation (2.18).

CHAPTER: 3

3.1: Design of Experiments

Design of Experiments is a powerful statistical technique, which can be applied, in metal cutting experiments. A well-designed experiment can reduce substantially reduce the number of tests, and yet provide all of the essential information for a statistical analysis which will yield useful information.

In the present work, factorial design has been adopted. A factorial design is one in which we control several factors and investigate their effects at each of two or more levels. The experimental design consists of making observation at each of all possible combinations that can be formed for the different levels of the factors. The approach in a factorial experiment is much different than in the traditional experiments, in which all factors but one are held constant. [36]

In the present work, 3^3 factorial design has been adopted. The three parameters which are involved are rotational speed (N), feed per revolution (f) and depth of cut (d). These three factors are each varied at three levels namely the lowest, intermediate and highest levels. These levels are set depending on the capacity of the machine and practical experience. Initial trial readings are taken to check whether the levels are set appropriately.

For the first set, where HSS with 10% Co was used as the tool material and EN24 steel was used as the work piece material, the parameters were set as follows:

Speed (N) (RPM): 32, 80 , 125.

Feed (f) (mm/revolution): 0.1, 0.15, 0.2

Depth of cut (mm): 1, 1.5 2.0

For the second set, where WC tool bit was used and EN24 steel was used as the work piece material, the cutting parameters were set as follows:

Speed (N) (RPM): 125, 160, 200.

Feed (f) (mm/revolution): 0.2, 0.25, and 0.3.

Depth of cut (mm): 1, 1.5, and 2.0.

Since speed has the greatest effect on the temperature generated and consequently the tool failure, as compared to the other two parameters, the selection of the maximum speed limit was of importance. Also beyond the maximum limit, there was the possibility of the mercury of the bath from spilling over.

The 3^3 design results in 27 experiments. The output of the experiments is the temperature (θ), which was recorded in terms of the voltage (mv) on the voltage recorder.

A general relation relating the output (y) with the input parameters ($x_1, x_2, \text{ and } x_3$) where the second order interaction among the parameters is assumed to be present is given by:

$$y = b_0 + b_1x_1 + b_2x_2 + b_3x_3 + b_{11}x_1^2 + b_{22}x_2^2 + b_{33}x_3^2 + b_{12}x_1x_2 + b_{23}x_2x_3 + b_{31}x_3x_1 \quad (3.1)$$

In this work θ is the output parameter measured in degree centigrade (C°) and x_1, x_2, x_3 are the speed, feed and depth of cut []

The b_0, b_1, \dots, b_i in the above equation are the regression coefficients which are the unknowns. The x_1^2, x_2^2, x_3^2 are the quadratic effects of the 3 variables and x_1x_2, x_2x_3 and x_3x_1 are the interaction effects.

Table 3.1 The factors set according to the 3^3 factorial design (HSS vs EN24 Steel)

Sl No	x_0	x_1	x_2	x_3	x_1^2	x_2^2	x_3^2	x_1x_2	x_2x_3	x_3x_1	θ
1	1	-1	-1	-1	1	1	1	1	1	1	
2	1	-1	-1	0.17	1	1	0.0289	1	-0.17	-0.17	
3	1	-1	-1	1	1	1	1	1	-1	-1	
4	1	-1	0.17	-1	1	0.0289	1	-0.17	-0.17	1	
5	1	-1	0.17	0.17	1	0.0289	0.0289	-0.17	0.0289	-0.17	
6	1	-1	0.17	1	1	0.0289	1	-0.17	0.17	-1	
7	1	-1	1	-1	1	1	1	-1	-1	1	
8	1	-1	1	0.17	1	1	0.0289	-1	0.17	-0.17	
9	1	-1	1	1	1	1	1	-1	1	-1	
10	1	0.344	-1	-1	0.118	1	1	-0.344	1	-0.344	
11	1	0.344	-1	0.17	0.118	1	0.0289		-0.17	0.0584	
12	1	0.344	-1	1	0.118	1	1	-0.344	-1	0.344	
13	1	0.344	0.17	-1	0.118	0.0289	1	0.0584	-0.17	-0.344	
14	1	0.344	0.17	0.17	0.118	0.0289	0.0289	0.0584	0.0289	0.0584	
15	1	0.344	0.17	1	0.118	0.0289	1	0.0584	0.17	0.344	
16	1	0.344	1	-1	0.118	1	1	0.344	-1	-0.344	
17	1	0.344	1	0.17	0.118	1	0.0289	0.344	0.17	0.0544	
18	1	0.344	1	1	0.118	1	1	0.344	1	0.344	
19	1	1	-1	-1	1	1	1	-1	1	1	

20	1	1	-1	0.17	1	1	0.0289	-1	-0.17	0.17	
21	1	1	-1	1	1	1	1	-1	-1	1	
22	1	1	0.17	-1	1	1	1	0.17	-0.17	-1	
23	1	1	0.17	0.17	1	1	0.0289	0.17	0.0289	0.17	
24	1	1	0.17	1	1	1	1	0.17	0.17	1	
25	1	1	1	-1	1	1	1	1	-1	-1	
26	1	1	1	0.17	1	1	0.0289	1	0.17	0.17	
27	1	1	1	1	1	1	1	1	1	1	

Table 3.2 The factors set according to the 3^3 factorial design (WC vs EN24 Steel)

Sl No	x_0	x_1	x_2	x_3	x_1^2	x_2^2	x_3^2	x_1x_2	x_2x_3	x_3x_1	θ
1	1	-1	-1	-1	1	1	1	1	1	1	
2	1	-1	-1	0.17	1	1	0.0289	1	-0.17	-0.17	
3	1	-1	-1	1	1	1	1	1	-1	-1	
4	1	-1	0.1	-1	1	0.01	1	-0.1	-0.1	1	
5	1	-1	0.1	0.17	1	0.01	0.0289	-0.1	0.17	-0.17	
6	1	-1	0.1	1	1	0.01	1	-0.1	0.1	-1	
7	1	-1	1	-1	1	1	1	-1	-1	1	
8	1	-1	1	0.17	1	1	0.0289	-1	0.17	-0.17	

9	1	-1	1	1	1	1	1	-1	1	-1	
10	1	0.05	-1	-1	0.0025	1	1	-0.05	1	-0.05	
11	1	0.05	-1	0.17	0.0025	1	0.0289	-0.05	-0.17	0.0085	
12	1	0.05	-1	1	0.0025	1	1	-0.05	-1	0.05	
13	1	0.05	0.1	-1	0.0025	0.01	1	0.005	-0.1	-0.05	
14	1	0.05	0.1	0.17	0.0025	0.01	0.0289	0.005	.017	0.0085	
15	1	0.05	0.1	1	0.0025	0.01	1	0.005	0.1	0.05	
16	1	0.05	1	-1	0.0025	1	1	0.05	-1	-0.05	
17	1	0.05	1	0.17	0.0025	1	0.0289	0.05	0.17	0.0085	
18	1	0.05	1	1	0.0025	1	1	0.05	1	-0.05	
19	1	1	-1	-1	1	1	1	-1	1	-1	
20	1	1	-1	0.17	1	1	0.0289	-1	-0.17	0.17	
21	1	1	-1	1	1	1	1	-1	-1	1	
22	1	1	0.1	-1	1	0.01	1	0.1	-0.1	-1	
23	1	1	0.1	0.17	1	0.01	0.0289	0.1	.017	0.17	
24	1	1	0.1	1	1	0.01	1	0.1	0.1	1	
25	1	1	1	-1	1	1	1	1	-1	-1	
26	1	1	1	0.17	1	1	0.289	1	0.17	0.17	
27	1	1	1	1	1	1	1	1	1	1	

The regression coefficients are evaluated by the following general equation

$$b_i = [XX']^{-1} X'y \quad (3.2)$$

Where $[X]$ is the matrix of the input parameters and y is the corresponding output. The output will be a $[10 \times 1]$ column vector representing the regression coefficients. [27]

3.2.Experimental Procedure: The experimental set up involved setting up the thermo-couple between the cutting tool and the work piece. Herbert-Gottwein thermocouple, which is also known as the dynamic thermocouple

has been used in the present work. The schematic diagram of the experimental set-up is shown in Figure 3.1

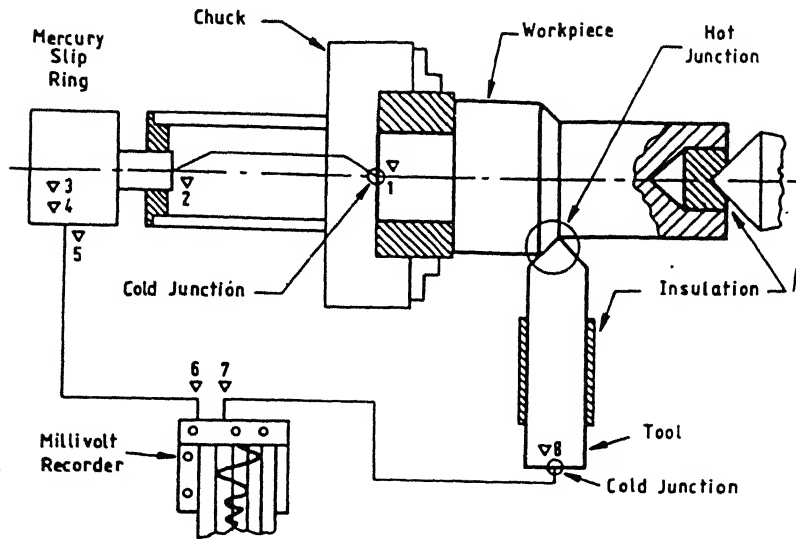


Figure 3.1. Experimental set up used for temperature measurement

A mild steel rod was attached to one end of the work piece was drilled and a screw rod was attached to it. The other end of the rod was dipped in a mercury bath by means of the slip ring. This is done to ensure continuous contact between the tool and the work piece during machining. One lead was taken from the mercury bath and the other lead was taken from the base of the cutting tool (in case of HSS). The tool and the work piece were insulated from the rest of the machine tool body. This was done by inserting insulating paper into the tailstock of the lathe. In order to insulate the tool on the tool post, it was mounted with insulating pieces at the bottom and at the side. The side packing also ensured that the tool was mounted perpendicular to the work piece. The two leads were connected to the millivolt recorder by through a switch. The recorder was switched on only when steady cutting conditions prevailed in the cutting zone. This was done to ensure that the recording pen does not travel arbitrarily when the circuit was closed.

The tool flank wear was measured after each reading by means of a traveling microscope, which has a least count of 0.0635mm. Proper lighting was provided during the observations.

3.3 Calibration Procedure: The calibration procedure involves finding the relation between the millivoltage generated during the cutting and the temperature existing in the cutting zone. There are different methods of calibration. The most commonly used method is the furnace type of calibration.

For the present work, a small portion of the work piece was welded to the cutting tool. This welded part of the work tool combination was dipped in the lead bath. The probe of the temperature recorder was also dipped in the bath. One lead from the tool and the other from the work piece were connected to the millivolt recorder. The temperature of the molten lead as indicated by the digital temperature recorder was noted at an interval of 10°C from 25°C to 200°C. The corresponding voltages in mv generated due to the thermocouple formed at the welded junction were noted for each temperature. Then the graph relating the temperature θ and voltage (mv) was obtained.

In case of Tungsten Carbide (WC), the tool tip was brazed to the work piece. Because of the possibility of melting of the insulated copper wire, bare copper wire was used. One lead was brazed to the tool bit and another lead was brazed to the work piece. The method of taking the readings was similar to that in case of HSS-EN24 steel calibration. Readings were taken both during the heating and cooling of lead and the most linear of the curves was used in subsequent experiments.

Chapter 4

4.1 Results of Calibration:

The calibration procedure as explained in the previous chapter yielded the results as shown in the curve in Fig 4.1a and Fig 4.1b. From the plot we can infer that there is almost a linear relation between the voltage generated during the machining and the corresponding temperature for the HSS tool and EN24 steel work piece combination and for the WC and EN24 steel combination.

4.2 Regression equation and its validity:

A general regression equation based on the least square estimation is established relating the input parameters and the corresponding output. As described in Chapter3, the general equation is given by equation (3.1)

In the present case,

$$\theta = b_0 + b_1N + b_2f + b_3d + b_{11}N^2 + b_{22}f^2 + b_{33}d^2 + b_{12}Nf + b_{23}fd + b_{31}dN \quad (4.1)$$

The bi's are the regression coefficients. Since 3^3 factorial design is used in the experiments the X matrix is a 27×10 matrix and the Y matrix is a 27×1 column vector. The regression coefficients are found by the relation

$$b_i = [X'X]^{-1} X'y \quad (4.2)$$

The output is a 10×1 column vector. The above equation was solved using MATLAB

The regression coefficients obtained are:

$$b_0 = 507.7516, b_1 = 152.9361, b_2 = 79.0231, b_3 = 25.3276, b_{11} = 92.9963 \\ b_{22} = 5.4916, b_{33} = 25.9698, b_{12} = 56.5985, b_{23} = -6.7562, b_{31} = 30.7667.$$

Thus the regression equation is given as

$$\begin{aligned} \theta = & 507.7516 + 152.9361(N) + 79.0231(f) + 25.3276(d) + 92.9963(N^2) \\ & + 5.4916(f^2) + 25.9698(d^2) + 56.5985(Nf) - 6.7562(fd) + 30.7667(dN) \end{aligned} \quad (4.3)$$

The regression equation gives the relation between the input parameters and the temperature, which is the output. In the above equation, the values of N , f and d are given in coded form. The coding is done as shown. [26]

$$x = \frac{2(\log_e A - \log_e A^+)}{(\log_e A^+ - \log_e A^-)} + 1 \quad (4.4)$$

In the above Equation A^+ is the maximum value of the parameter and A^- is the minimum value of the parameter. A is the intermediate value at which the coded value of the parameter is required.

The minimum and the maximum levels of the parameters are respectively -1 and $+1$ as can be seen from the above relation. In equation (4.4) x is the coded value of the variable. Since the cutting parameters available on the lathe are not exactly such as to give an intermediate level of the coded variable as zero, the intermediate level is coded as given below for the 3 parameters

$$\text{For speed, } x_v = \frac{2(\log_e 80 - \log_e 125)}{(\log_e 125 - \log_e 32)} + 1 \quad (4.5a)$$

$$x_v = 0.3449$$

$$\text{For feed, } x_f = \frac{2(\log_e 0.15 - \log_e 0.2)}{(\log_e 0.2 - \log_e 0.1)} + 1 \quad (4.5b)$$

$$x_f = 0.17$$

$$\text{For depth of cut, } x_d = \frac{2(\log_e 1.5 - \log_e 2)}{(\log_e 2 - \log_e 1)} + 1 \quad (4.5c)$$

$$x_d = 0.17$$

The values of the parameters and the corresponding temperatures (θ) and the flank wear land are given in table 4.1

The theoretical temperature as calculated by using the equation (4.3) is compared with the experimental temperatures and is shown in Table 4.2

In case of the Experiments with the WC tool bit the coded value of the intermediate variable is calculated using Equation (4.5)

$$N = 2 \frac{(\log_e 160 - \log_e 200)}{(\log_e 200 - \log_e 125)} + 1 = 0.05 \quad (4.5d)$$

$$f = \frac{2(\log_e 0.25 - \log_e 0.3)}{(\log_e 0.3 - \log_e 0.2)} + 1 = 0.1 \quad (4.5e)$$

$$d = \frac{2(\log_e 1.5 - \log_e 2.0)}{(\log_e 2.0 - \log_e 1.0)} + 1 = 0.17 \quad (4.5f)$$

Table 4.1 Input parameters and corresponding temperatures and flank wear

Sl No.	Speed (RPM)	Feed (mm/rev)	Depth of cut (mm)	Temperature	Flank wear (mm)
1	32	0.1	1	450	0.2540
2	32	0.1	1.5	467	0.2222
3	32	0.1	2.0	482	0.2857
4	32	0.15	1	486	0.3175
5	32	0.15	1.5	495	0.2540
6	32	0.15	2.0	495	0.2540
7	32	0.20	1	486	0.3810
8	32	0.20	1.5	495	0.3175
9	32	0.20	2.0	504	0.28575
10	80	0.1	1	485	0.41275
11	80	0.1	1.5	486	0.47625
12	80	0.1	2.0	567	0.60375
13	80	0.15	1	585	0.6350
14	80	0.15	1.5	603	0.6985
15	80	0.15	2.0	641	0.8255
16	80	0.20	1	666	0.85725
17	80	0.20	1.5	675	0.92075
18	80	0.20	2.0	720	1.016
19	125	0.1	1	612	0.5080

20	125	0.1	1.5	621	0.41275
21	125	0.1	2.0	783	0.6350
22	125	0.15	1	792	0.6350
23	125	0.15	1.5	810	0.7620
24	125	0.15	2.0	846	0.8890
25	125	0.2	1	873	1.5875
26	125	0.2	1.5	918	1.0795
27	125	0.2	2.0	963	1.7145

Table 4.2 Theoretical and Experimental values of temperature

No	Theoretical Temperature	Experimental Temperature
1	455.53	450
2	432.23	467
3	458.16	482
4	484.34	486
5	451.41	495
6	471.16	495
7	513.89	486
8	474.40	495
9	489.50	504
10	461.63	485
11	486.33	486
12	546.93	567
13	579.44	585
14	594.40	603
15	648.96	641
16	672.13	666
17	681.02	675
18	730.57	720
19	648.20	612
20	634.98	621
21	712.37	783
22	747.92	792
23	786.98	810
24	857.81	846
25	871.42	873
26	929.47	918
27	970.10	963

From the Table 4.2 we see that the experimental and the theoretical values are comparable. The flank wear is calculated using the relation (2.18) and is compared with the experimental values of the flank wear as shown in Table 4.3.

Table 4.3 Theoretical and Experimental Flank Wear h_f :

Sl No	Theoretical Value	Experimental Value
1	0.2394	0.2540
2	0.2154	0.2222
3	0.2420	0.2857
4	0.2705	0.3175
5	0.2349	0.2540
6	0.2560	0.2540
7	0.3045	0.3810
8	0.2595	0.3175
9	0.2763	0.28575
10	0.3990	0.41275
11	0.4428	0.47625
12	0.5600	0.60325
13	0.6286	0.6350
14	0.6626	0.6985
15	0.7885	0.8255
16	0.8458	0.85725
17	0.8684	0.92075
18	0.9993	1.016
19	0.4962	0.5080
20	0.4761	0.41275
21	0.5993	0.635
22	0.6606	0.6350
23	0.7314	0.7620
24	0.8690	0.8890
25	0.8968	1.5875
26	1.0202	1.0795
27	1.1111	1.7145

To find the value of K_f in equation (2.18), the output (h_f) theoretical is assumed to be related to the input parameters (N, f and d) similar as in the case of temperature.

The value of K_f is calculated as:

$$K_f = \frac{h_f * V_c}{\theta_f^2} \quad (4.6)$$

The Regression equation where the flank wear land h_f is assumed to be related to the input parameters is found out by using equation (4.2) where the y column vector represents the measured flank wears (as given in Table 4.3). The relation is given in equation (4.7)

$$h_f = 0.433 + 0.3029N + 0.2184f + 0.0435d - 0.128N^2 + 0.1273f^2 + 0.1115d^2 + 0.1993Nf - 0.0163fd + 0.0562dN.$$

(4.7)

4.3. Effect of various parameters on the temperature and the Flank wear land:

Figures 4.2, 4.3 and 4.4 show the effect of rotational speed on the temperature generated at various feeds. From the plots it can be observed that the temperature increases as the speed increases. This is because as the cutting speed is increased a greater quantity of material passes through the shear zone per unit time. The rate of heat generation is dependant on the amount of material entering the shear zone, which in turn is dependent on the cutting speed. At high speeds the rate of plastic deformation is correspondingly higher (thus increasing the temperature). The variation is nearly parabolic in nature. Also at higher depths of cut the curve shifts upwards-indicating higher temperatures. This is because as speed and depth of cut increases the rate of plastic deformation in the primary zone increases and this energy required for the plastic deformation is converted into heat energy, which is indicated by the temperature. At higher feeds of 0.15 and 0.2mm/rev, the trend is similar but the temperatures encountered are higher.

Effect of depth of cut on the temperature is shown in Figures 4.5. There is a linear increase in temperature as the depth of cut increases, with higher feeds giving rise to higher temperatures. When the depth of cut is increased the shear zones are also proportionately increased. This causes an increase in the amount of heat generated and hence higher temperatures are observed. Figures 4.6 and 4.7 shows the variation of temperature with of depth of cut at higher speeds. Though

the depth of cut has the least effect on the temperature its effect is significant from the point of view of tool wear in combination with the other two parameters.

Figures 4.8, 4.9 and 4.10 show the variation of temperature with feed. The variation is nearly parabolic in nature similar to the variation with speed. Higher speeds and depth of cut results in higher temperatures. As the feed rate is increased the quantity of material removed per unit time is correspondingly increased. On account of this increase, the rate of shearing of the work piece is also increased.

For the same depth of cut, from Figure 4.2 and 4.9 we observe that temperature variation is more sensitive to the speed than to the feed. This compares well with the previous works, which indicate that speed has greater effect on temperatures than the feed.

Figure 4.12a, 4.12b, 4.12c, 4.13a, 4.13b, 4.13c and 4.14a, 4.14b and 4.13c show the variation of flank wear land h_f with the flank temperatures at different feeds and speeds. The curves are linear which agrees well with the results of growth of wear land in the steady state region.

4.4 Effect of various input parameters on temperatures and flank wear (WC vs. EN24)

For the experiments with WC tool bits the parameters were set at a higher level as given in Chapter 3. The parameters set as per the factorial design is given in the coded form in Table 3.2.

Regression equation based on the least square estimation is used to relate the input parameters with the output. The regression coefficients are calculated using the formula given in (4.3). The regression equation obtained is

$$\begin{aligned} \theta = & 713.143 + 32.7208N + 34.3789f + 14.4224d - 3.6082N^2 + 3.447f^2 \\ & + 2.2711d^2 + 1.1133Nf + 2.4037fd - 2.7863dN \end{aligned} \quad (4.8)$$

Value of the constant K_f is calculated in the same way as in the case of the HSS tool experiments. The value of the constant obtained is 5, which is an

average value of the 27 trials. The theoretical and the experimental temperatures are as given in Table 4.3

The regression equation where the flank wear is assumed to be related to the input parameters is

$$h_f = 0.1209 - 0.0017N + 0.0194f + 0.0139d - 0.0054N^2 + 0.0073f^2 - 0.0003d^2 - 0.0025Nf + 0.0006fd - 0.0004dN \quad (4.9)$$

Table 4.4 Input parameters and corresponding Temperature and Flank Wear.

Sl. No.	Speed (N)	Feed(mm/rev)	Depth Of cut (mm)	Temperature	Flank wear
1	125	0.2	1.0	619.4	0.09525
2	125	0.2	1.5	652	0.09525
3	125	0.2	2.0	668.3	0.1270
4	125	0.25	1.0	668.3	0.09525
5	125	0.25	1.5	684.6	0.1270
6	125	0.25	2.0	700.9	0.1270
7	125	0.3	1.0	700.9	0.1270
8	125	0.3	1.5	717.2	0.15875
9	125	0.3	2.0	733.5	0.15875
10	160	0.2	1.0	684.6	0.09525
11	160	0.2	1.5	684.6	0.09525
12	160	0.2	2.0	700.9	0.1270
13	160	0.25	1.0	717.2	0.1270
14	160	0.25	1.5	717.2	0.1270
15	160	0.25	2.0	733.5	0.1270
16	160	0.3	1.0	733.5	0.1270
17	160	0.3	1.5	749.8	0.15875
18	160	0.3	2.0	766.1	0.15875
19	200	0.2	1.0	700.9	0.09525
20	200	0.2	1.5	717.2	0.09525
21	200	0.2	2.0	717.2	0.1270
22	200	0.25	1.0	733.5	0.09525
23	200	0.25	1.5	749.8	0.1270
24	200	0.25	2.0	749.8	0.1270
25	200	0.3	1.0	766.1	0.1270
26	200	0.3	1.5	782.4	0.1270
27	200	0.3	2.0	815.0	0.15875

Table 4-5 Theoretical and Experimental Temperatures for WC vs. EN24 Steel.

Sl No.	Theoretical temperature	Experimental Temperature
1	634.96	619.4
2	649.49	652
3	663.56	668.3
4	665.50	684.6
5	683.12	700.9
6	699.38	700.9
7	696.69	700.9
8	716.84	717.2
9	734.90	733.5
10	671.53	684.6
11	685.87	684.6
12	697.95	700.9
13	715.97	717.2
14	720.78	717.2
15	735.29	733.5
16	738.21	749.8
17	755.55	766.1
18	701.63	700.9
19	702.74	717.2
20	711.93	717.2
21	722.22	717.2
22	735.72	733.5
23	751.79	749.8
24	760.49	749.8
25	768.91	766.1
26	783.73	782.4
27	800.92	815.4

. In case of the Carbide tool bit the input parameters were set at a higher level as described in Chapter 3. The parameters set according to the factorial design is given in Table 32.

Table 4.6 Experimental and theoretical values of flank wear land. (WC vs EN24 Steel)

Sl No.	Theoretical flank Wear	Experimental flank Wear
1	0.0886	0.09525
2	0.0977	0.09525
3	0.116	0.1270
4	0.1070	0.09525
5	0.12189	0.1270
6	0.13012	0.1270
7	0.1443	0.1270
8	0.1455	0.15875
9	0.1610	0.15875
10	0.09524	0.09525
11	0.1110	0.09525
12	0.12197	0.1270
13	0.12286	0.1270
14	0.12525	0.1270
15	0.1360	0.1270
16	0.1331	0.1270
17	0.1498	0.15875
18	0.1506	0.15875
19	0.0910	0.09525
20	0.1063	0.09525
21	0.1168	0.1270
22	0.1292	0.09525
23	0.1178	0.1270
24	0.1288	0.1270
25	0.1236	0.1270
26	0.1403	0.1270

4.4.a Effect of various parameters on temperature:

Figure 4.15, shows the effect of depth of cut on the temperature generated. The variation is almost linear with higher feeds giving higher temperatures. If we compare Figure 4.7, with the first curve of Figure 4.15 (cutting parameters are the same in both), the temperature is more in the first case. This is because the rate of tool wear in HSS tool is more than that of the WC tool bit. Figure 4.16 and 4.17 show the variation of temperature with depth of cut at 160RPM and 200 RPM respectively.

The effect of speed on the temperature at a given feed of 0.2mm per rev. is shown in Figure 4.18. Temperature increases with increasing depth of cut. The variation is parabolic in nature as in the case of HSS tool. Figures 4.19 and 4.20 gives the temperature variation at 0.25mm/rev and 0.3mm/rev feed. Comparison of Figure 4.4 with Figure 4.18 shows that higher temperatures are generated in case of HSS tool than the WC tool bit. This is because of the higher wear of HSS tool and also the composition of the tool (the tool contains 10% Cobalt).

Figures 4.21 to 4.23 show the variation of temperature with feed at 125RPM, 160 RPM and 200 RPM respectively. There is almost a linear relation between the feed and the temperature. Higher depths of cut results in higher temperatures.

4.4.b Effect of input parameters on Flank wear width h_f :

Figure 4.24 shows the effect of rotational speed on the flank wear land. For the three speeds used, the curves shift upwards-indicating higher temperatures. But the flank wear land remains almost the same for the three speeds. It can be observed that there is a linear increase in temperature as the wear land increases. At higher feeds of 0.25mm/rev and 0.3mm/rev the variation is the same, but the temperatures as well as the wear land are higher. (Figures 4.25 and 4.26).

The effect of depth of cut on the flank wear is minimal as can be observed from Figures 4.27, 4.28 and 4.29. Though there is an increase in temperature at higher depths of cut, the effect on flank wear is insignificant.

Olberts [13] conducted tests on AISI 1015 steel tube with NS-6 carbide tool. At various speeds and feeds, the variation of flank wear land with the interface temperature was examined. There was a linear variation in the plots. In the present work too, there is a linear increase in flank temperature with the flank wear. Hence we can infer that speed and feed affect the flank wear but the depth of cut has a negligible effect on the flank wear.

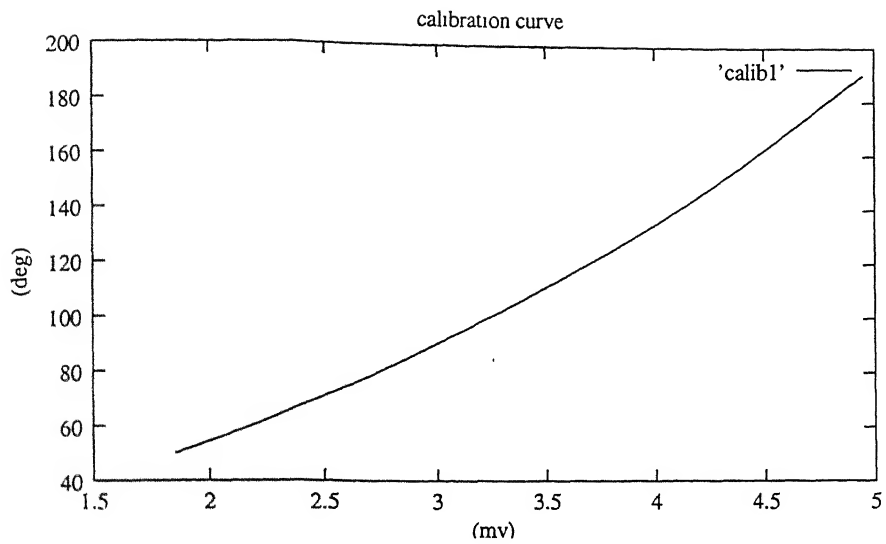


Figure 4.1a Calibration curve for HSS vs EN24 Steel

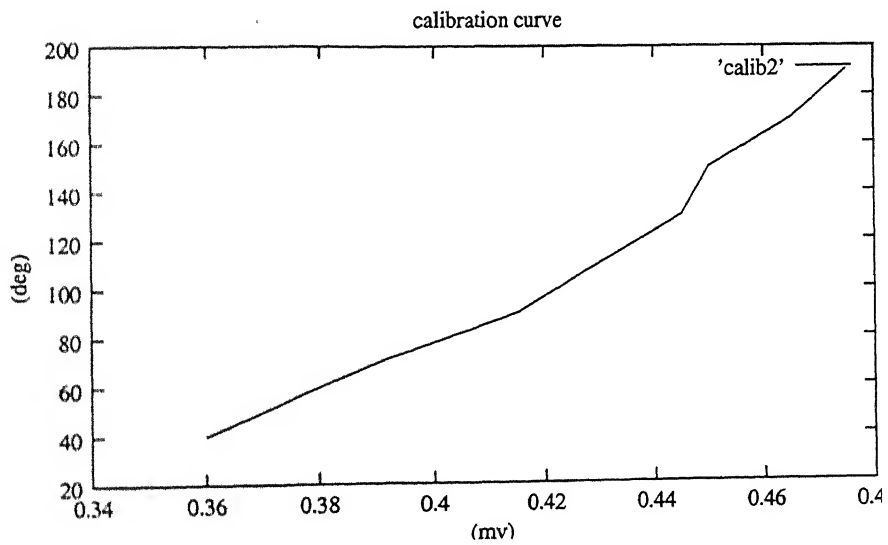


Figure 4.1b Calibration curve for WC vs EN24 Steel

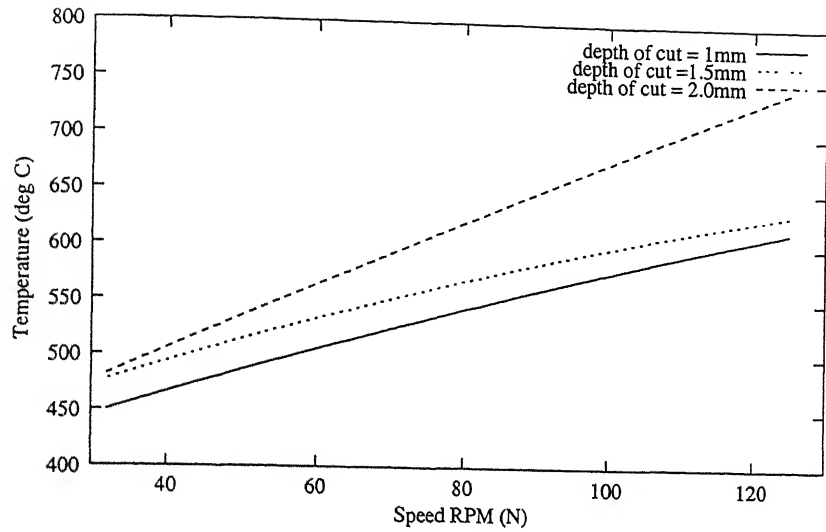


Figure 4.2 Variation of speed vs temperature at 0.1mm/rev feed

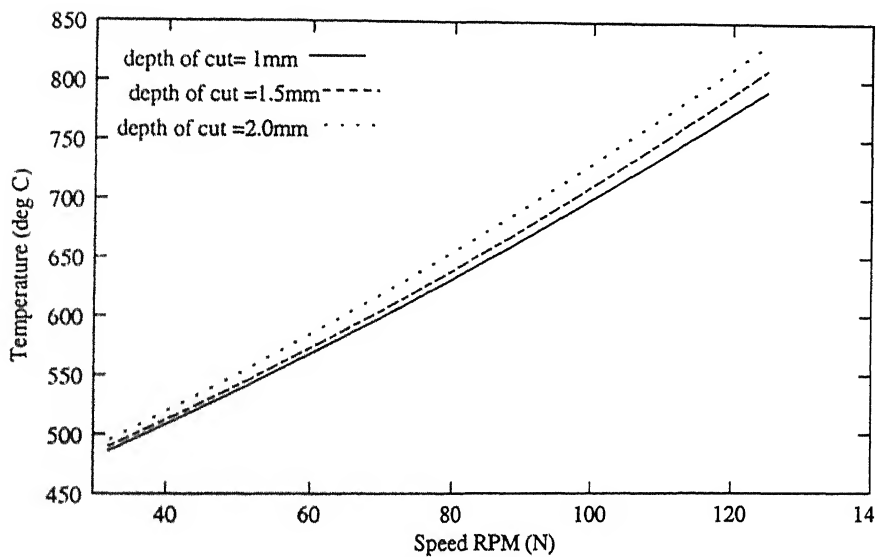


Figure 4.3 variation of speed vs temperature at 0.15mm/rev feed

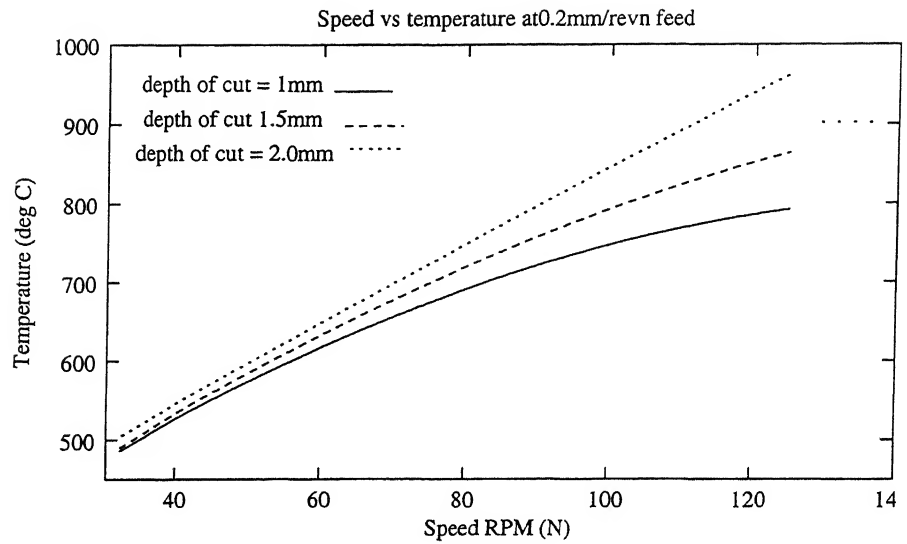


Figure 4.4 Variation of speed vs temperature at 0.2mm/rev feed

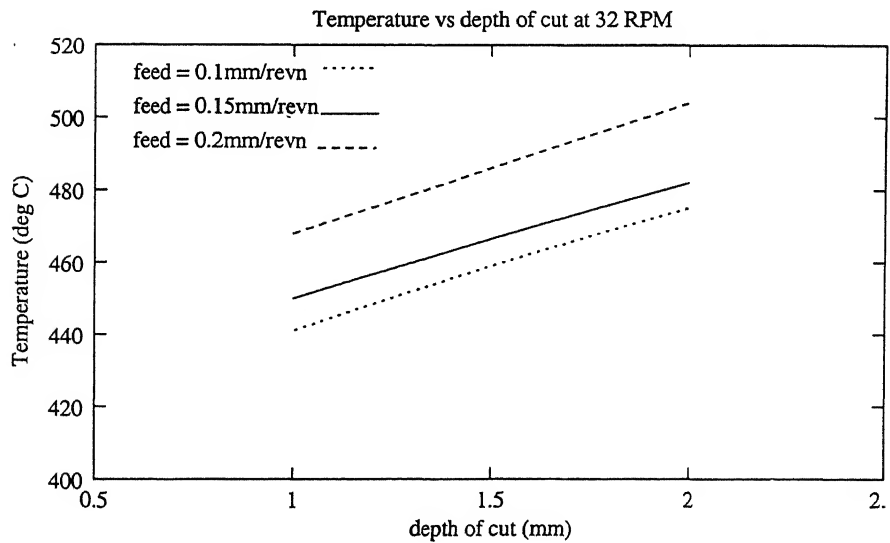


Figure 4.5 variation of temperature vs depth of cut at 32 RPM

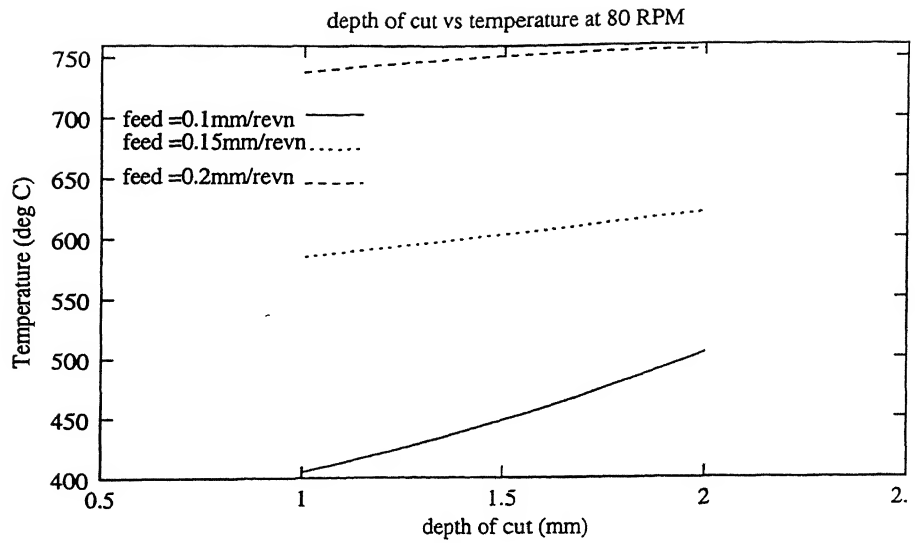


Figure 4.6 variation of temperature vs depth of cut at 80 RPM

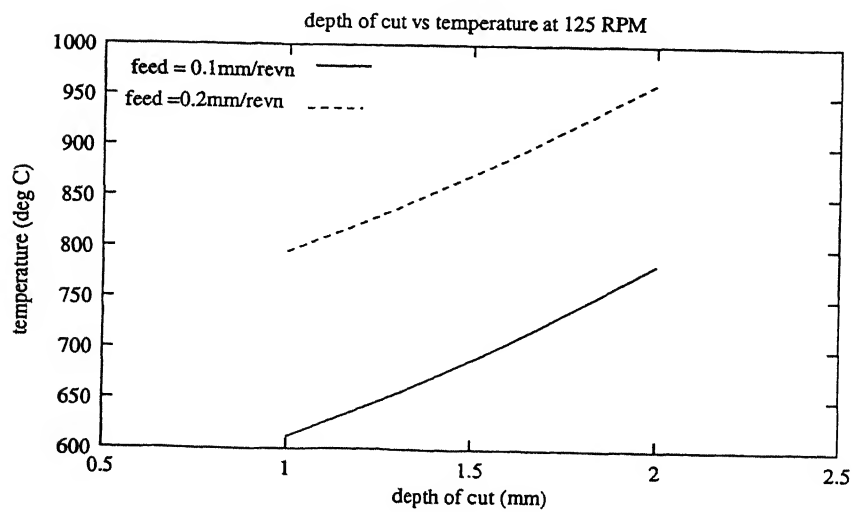


Figure 4.7 variation of temperature vs depth of cut at 125 RPM

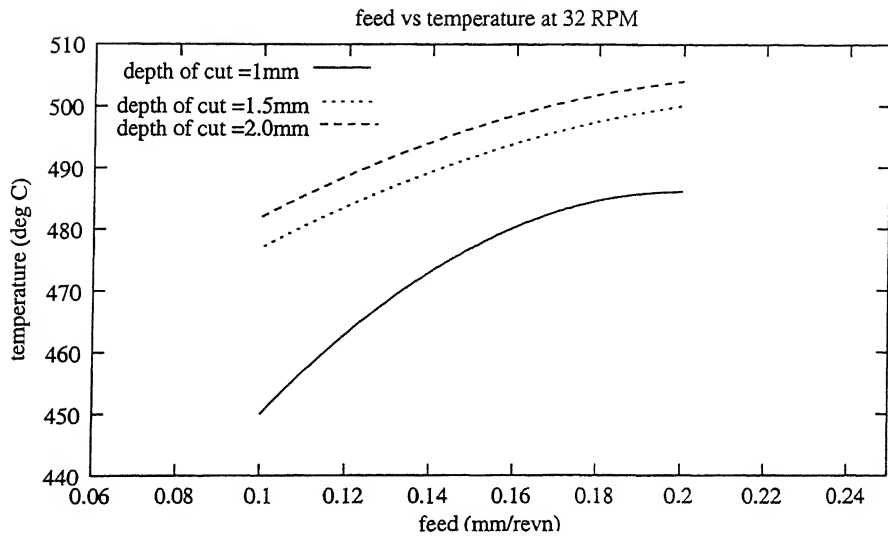


Figure 4.8 variation of temperature vs feed at 32 RPM

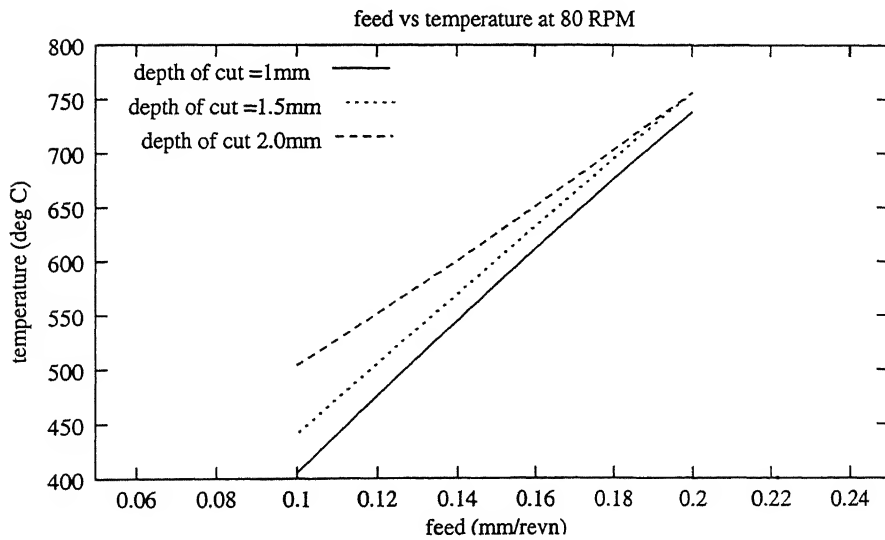


Figure 4.9 variation of temperature vs feed at 80 RPM

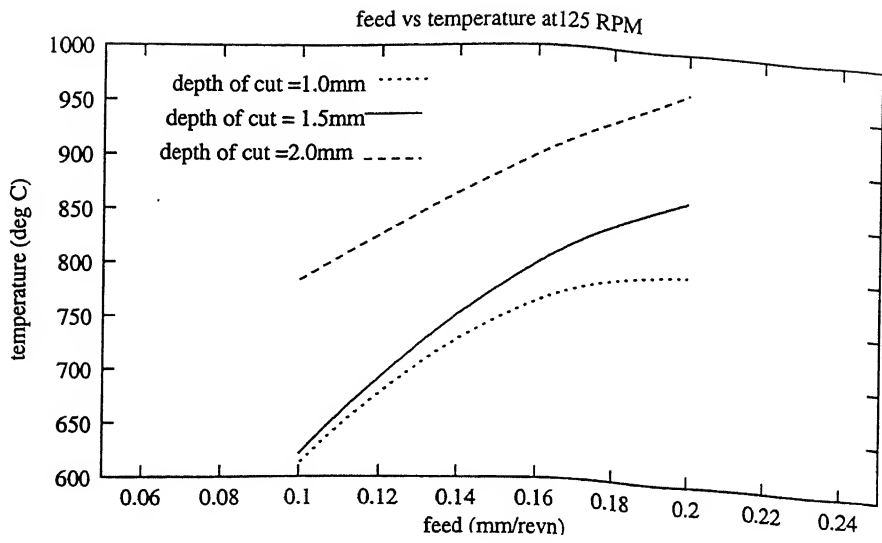


Figure 4.10 variation of temperature vs feed at 125 RPM

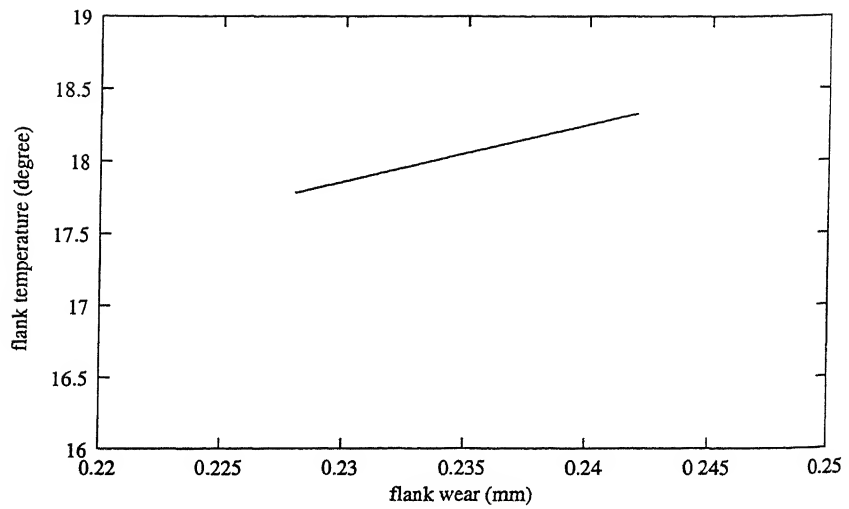


Figure 4.12a Variation of flank wear with flank temperature at 32 RPM and 0.1mm/rev feed

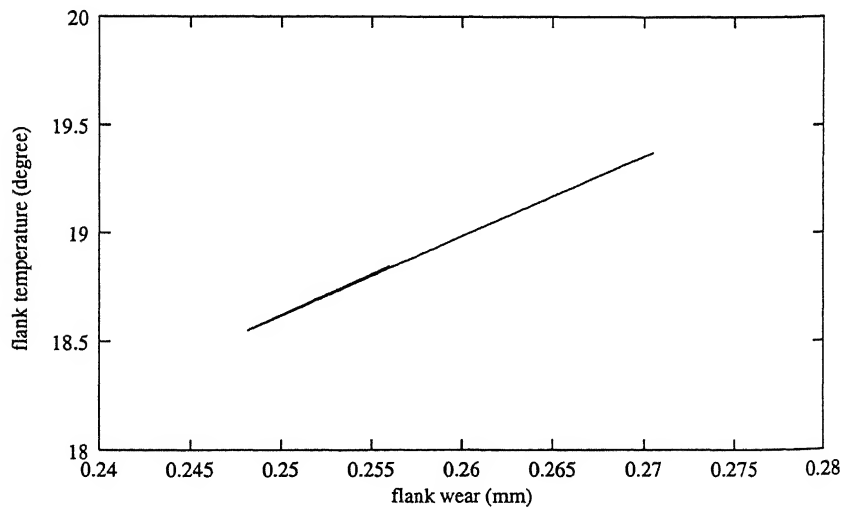


Figure 4.12b Variation of flank wear with flank temperature at 32 RPM and 0.15mm/rev feed

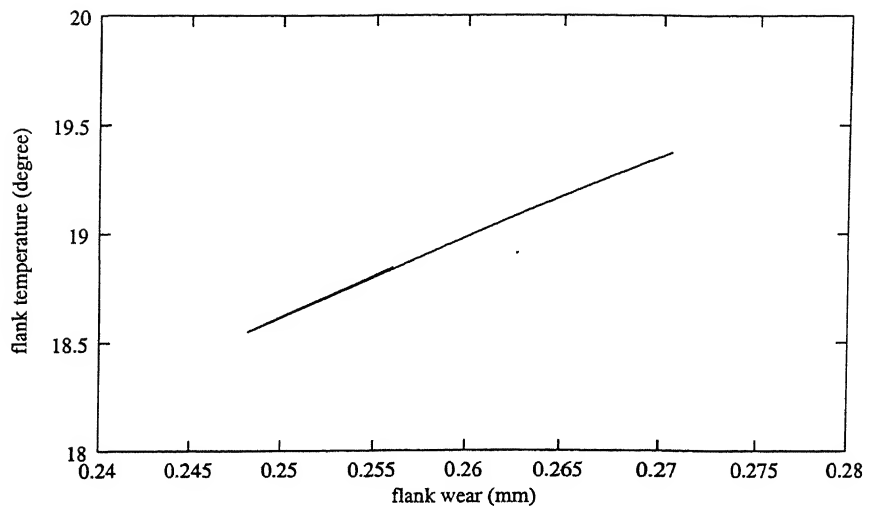


Figure 4.12c Variation of flank wear with flank temperature at 32 RPM and 0.2mm/rev feed

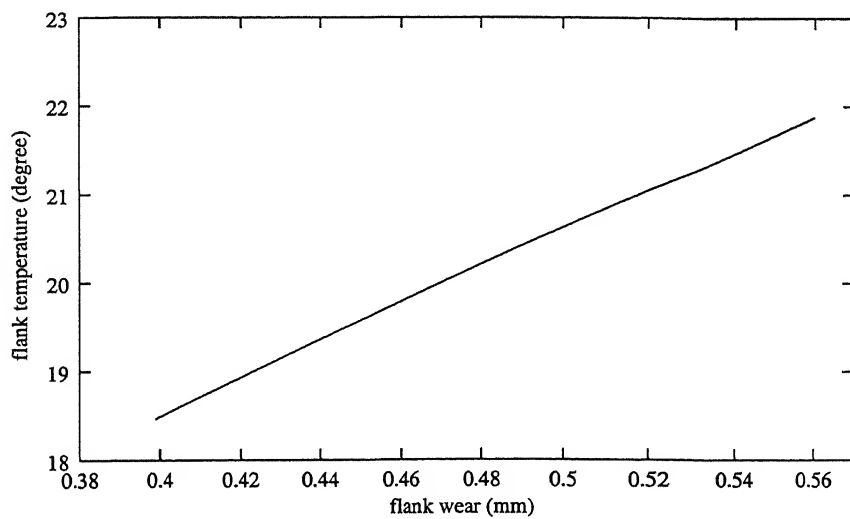


Figure 4.13a Variation of flank wear with flank temperature at 80 RPM and 0.1mm/rev feed

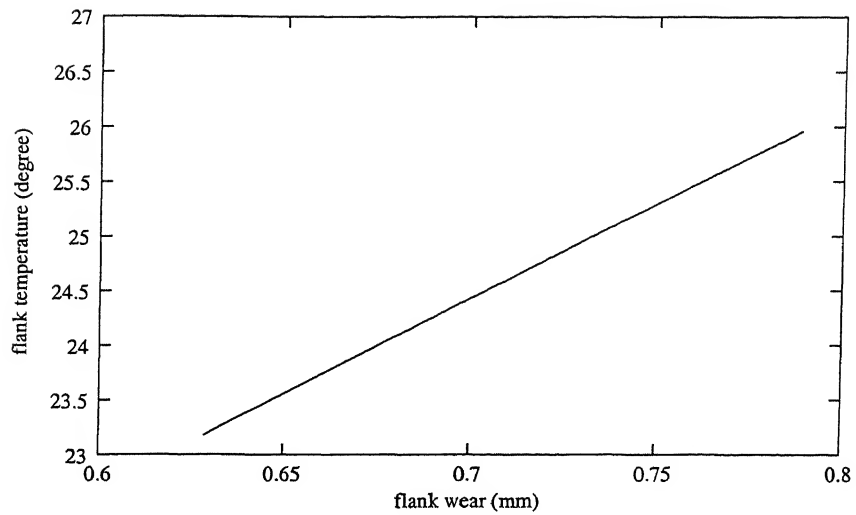


Figure 4.13b Variation of flank wear with flank temperature at 80 RPM and 0.15mm/rev feed

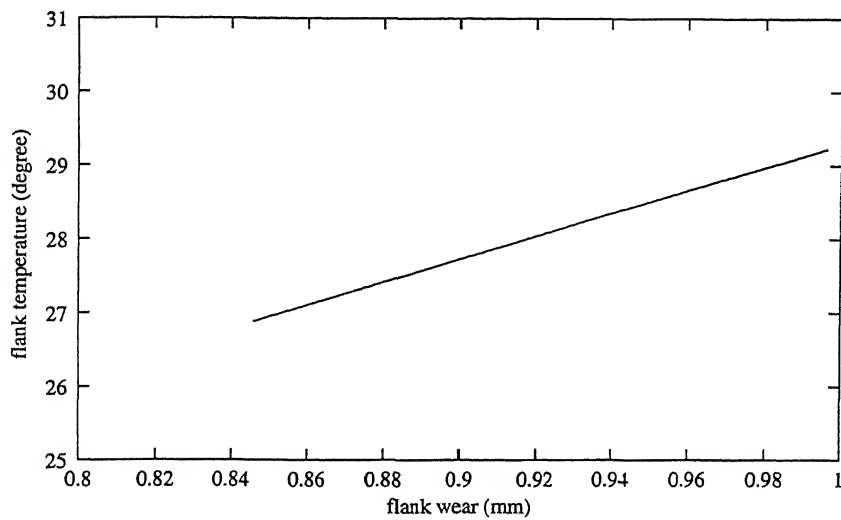


Figure 4.13c Variation of flank wear with flank temperature at 80 RPM and 0.2mm/rev feed

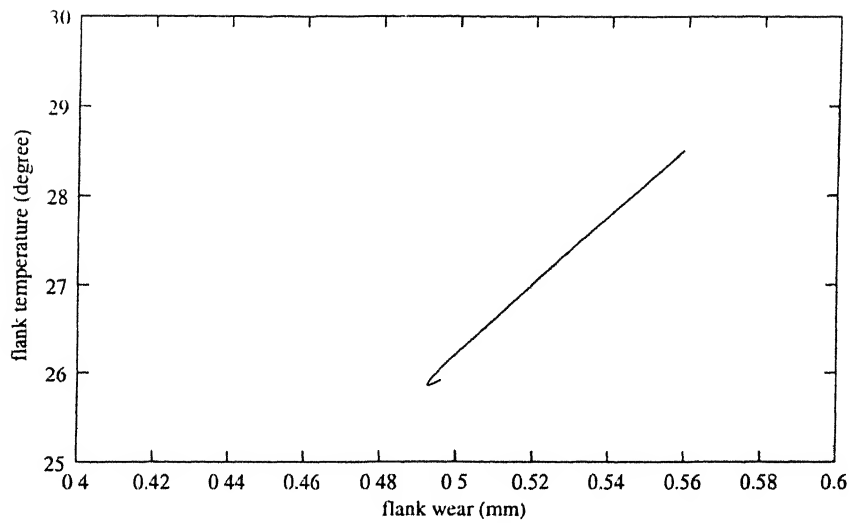


Figure 4.14a Variation of flank wear with flank temperature at 125 RPM and 0.1mm/rev feed

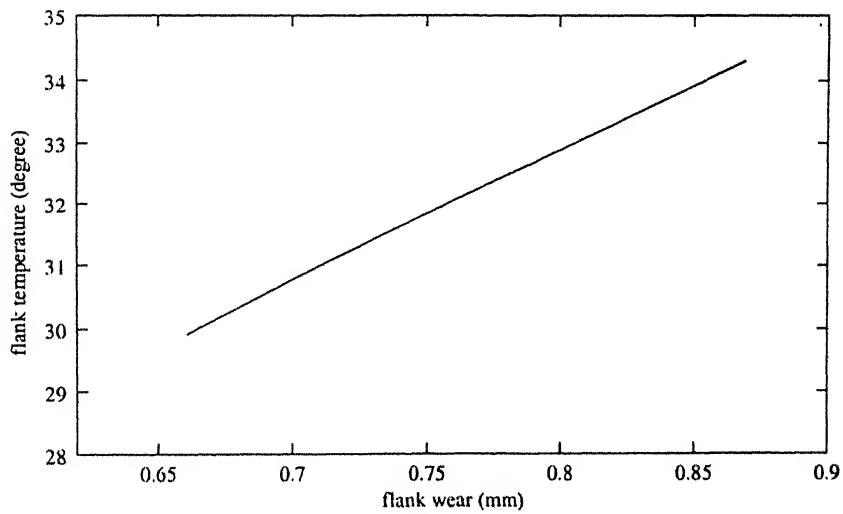


Figure 4.14b Variation of flank wear with flank temperature at 125 RPM and 0.15mm/revn feed

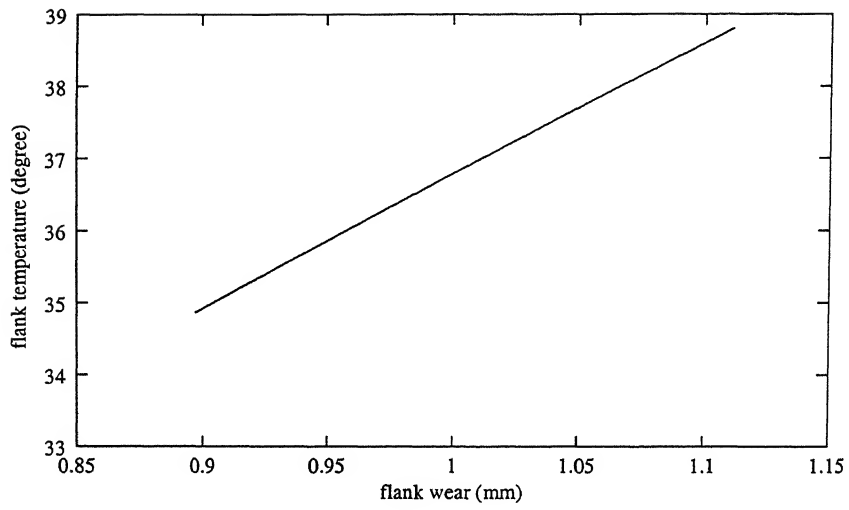


Figure 4.14c Variation of flank wear with flank temperature at 125 RPM and 0.2mm/revn feed

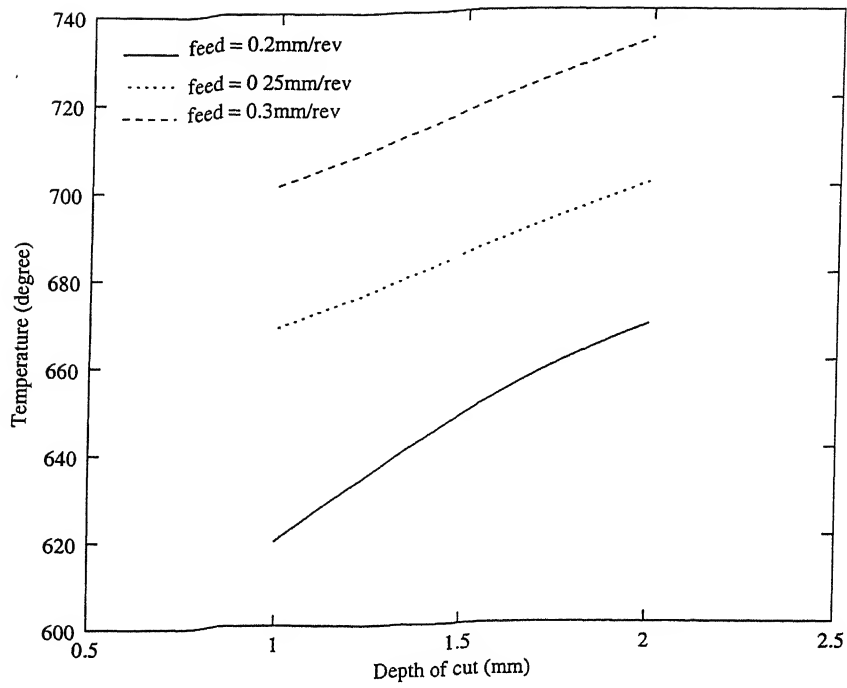


Figure 4.15 Variation of temperature with depth of cut at 125 RPM

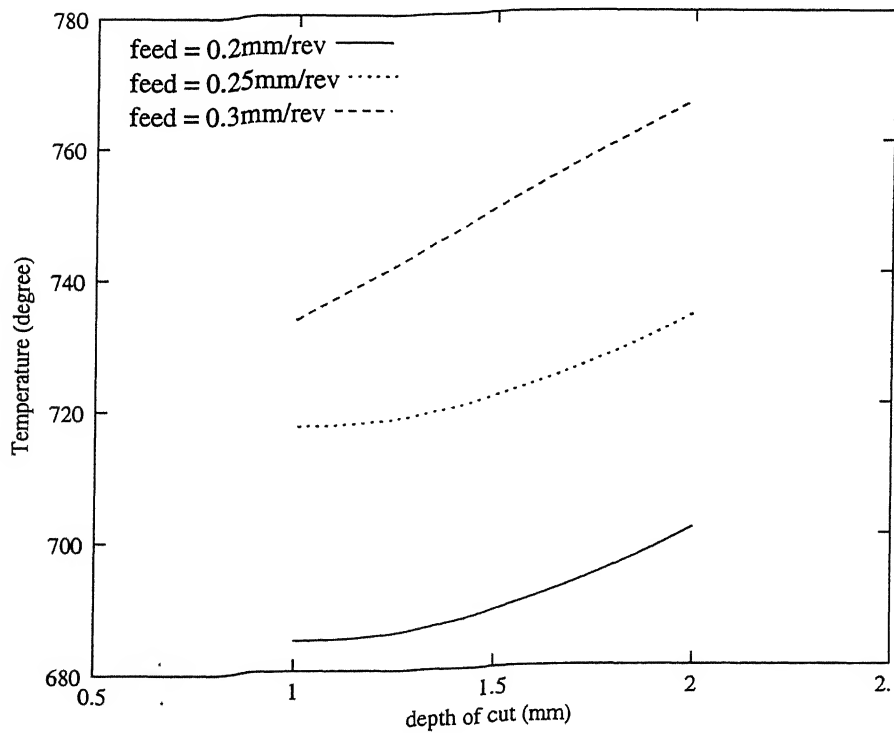


Figure 4.16 Variation of temperature with depth of cut at 160 RPM

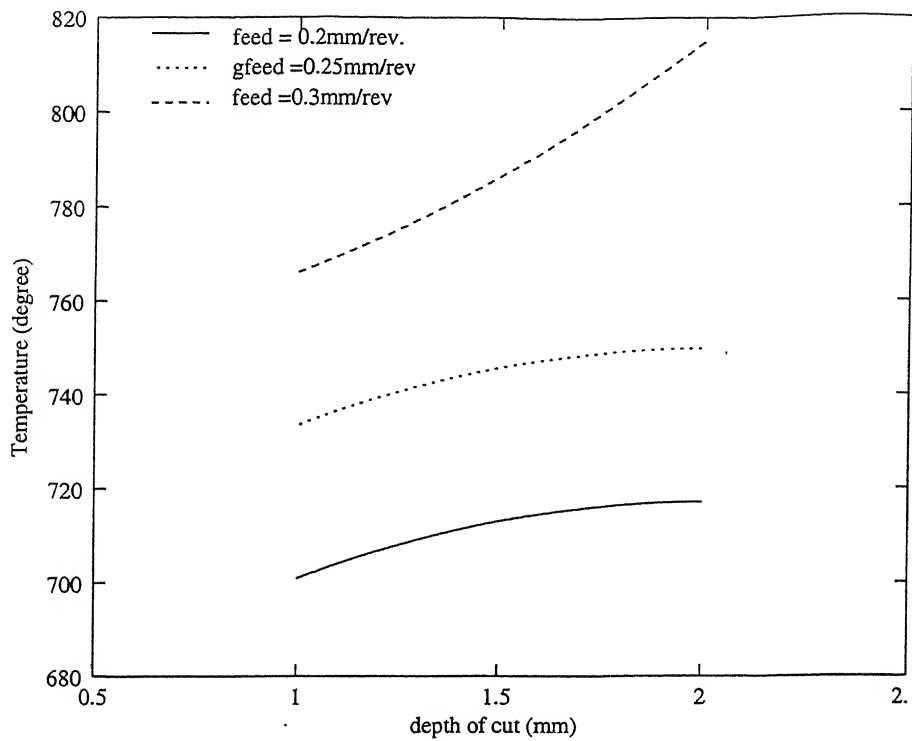


Figure 4.17 Variation of temperature with depth of cut at 200 RPM

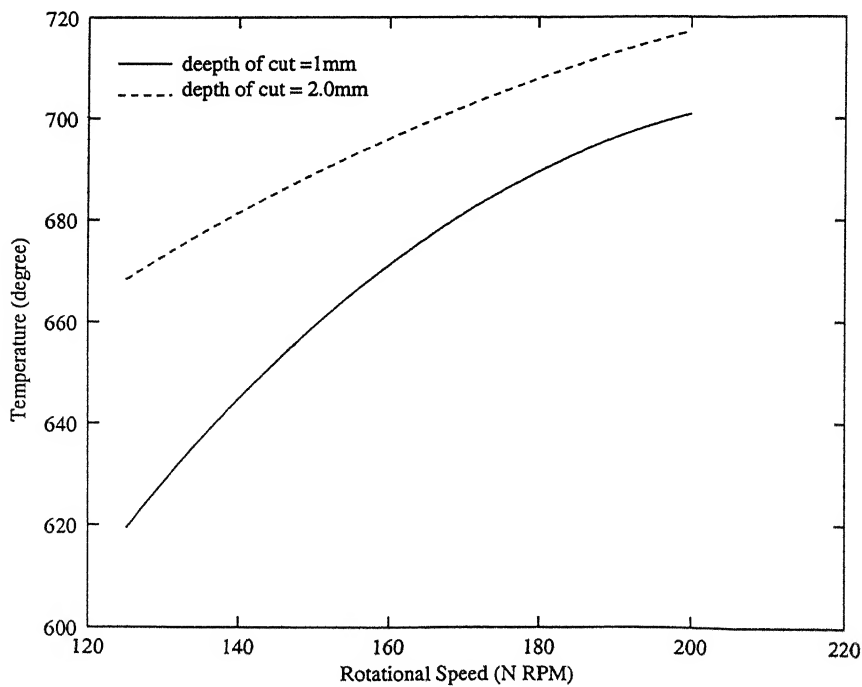


Figure 4.18 Variation of temperature with Rotational speed at 0.2mm/rev feed

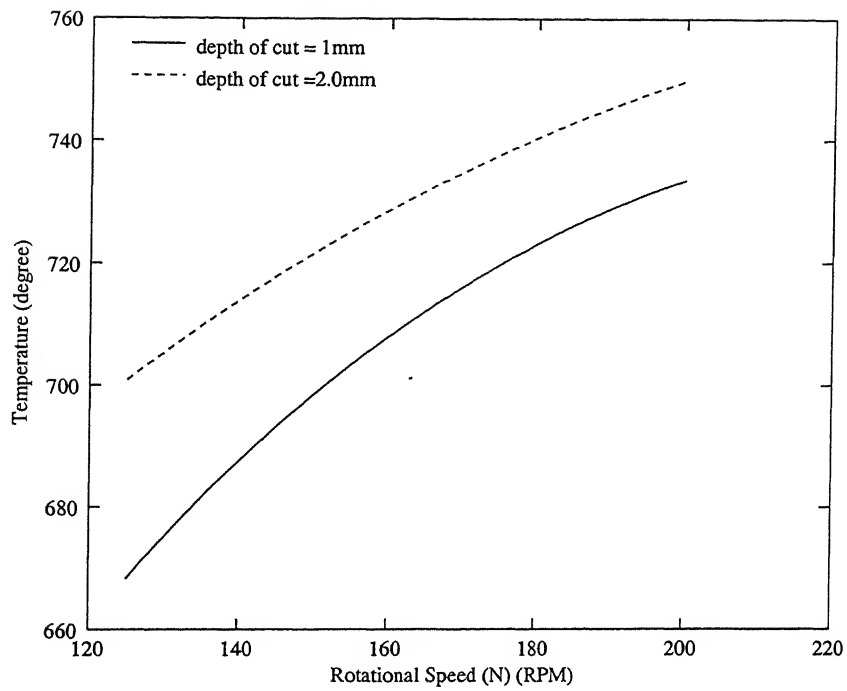


Figure 4.19 Variation of temperature with Rotational speed at 0.25mm/rev feed

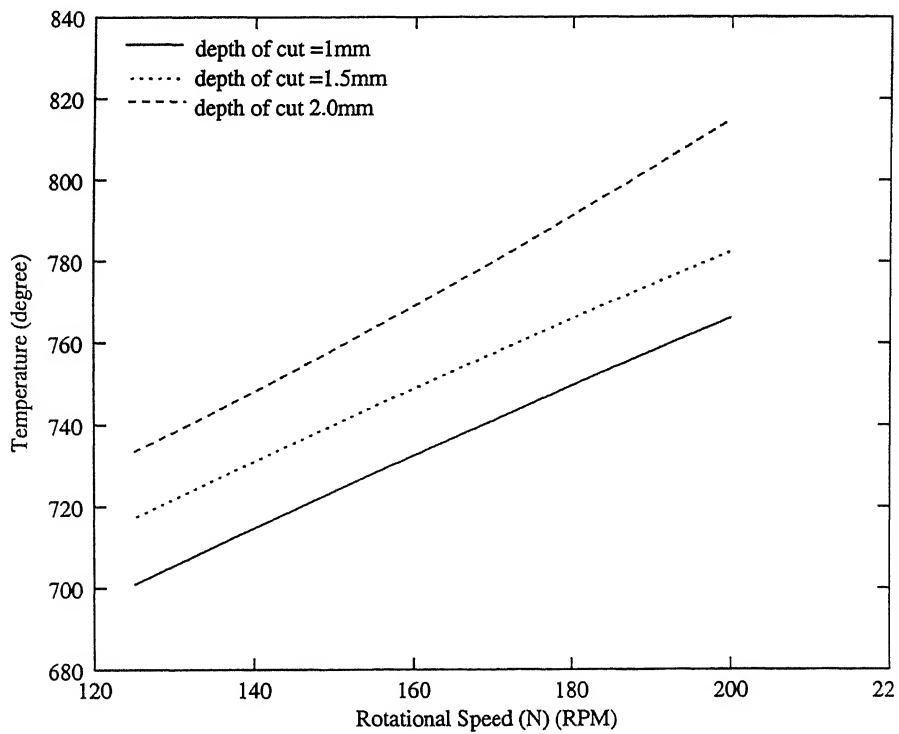


Figure 4.20 Variation of temperature with Rotational speed at 0.3mm/rev feed

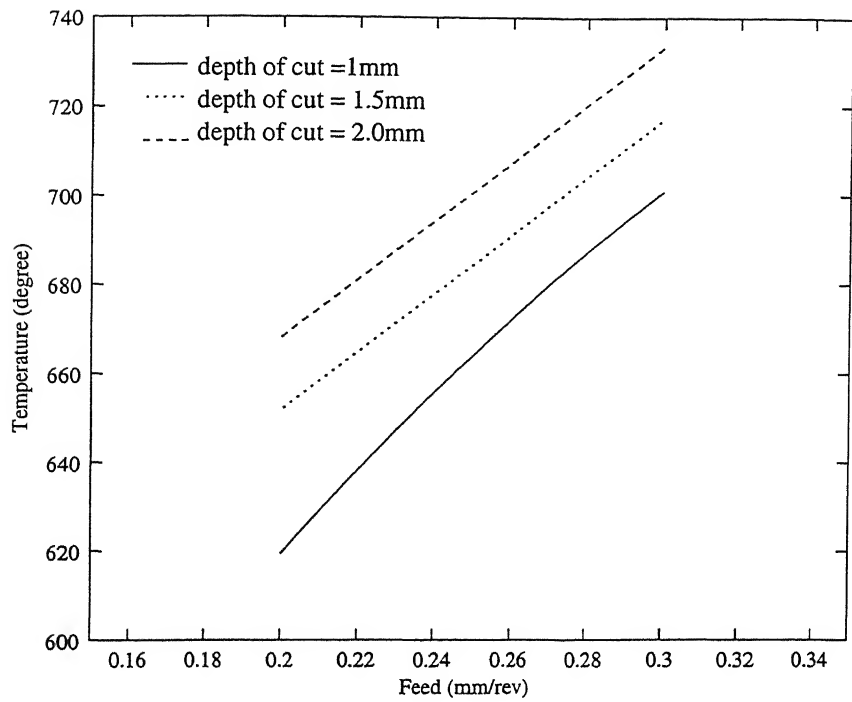


Figure 4.21 Variation of temperature with feed at 125 RPM

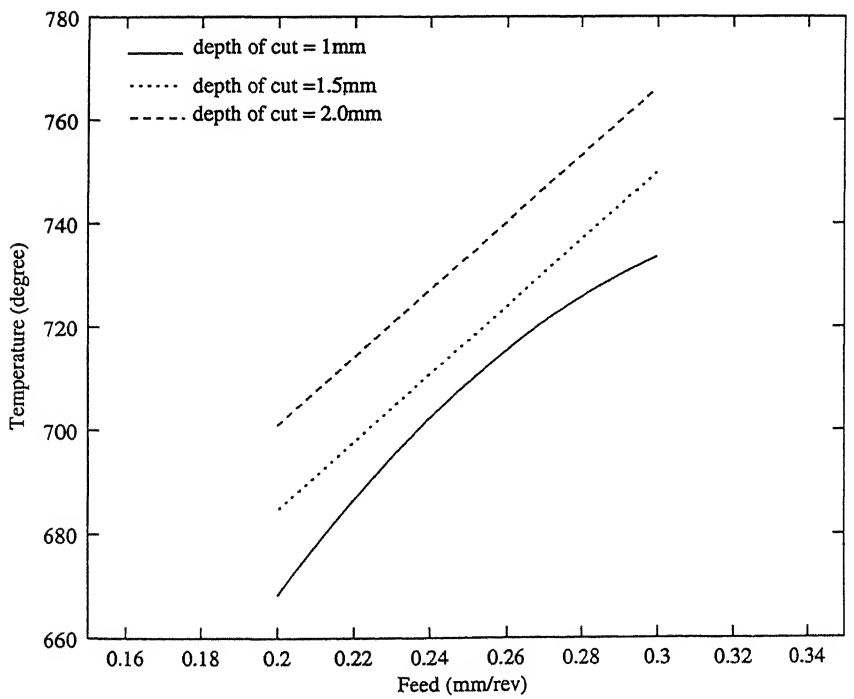


Figure 4.22 Variation of temperature with feed at 160 RPM

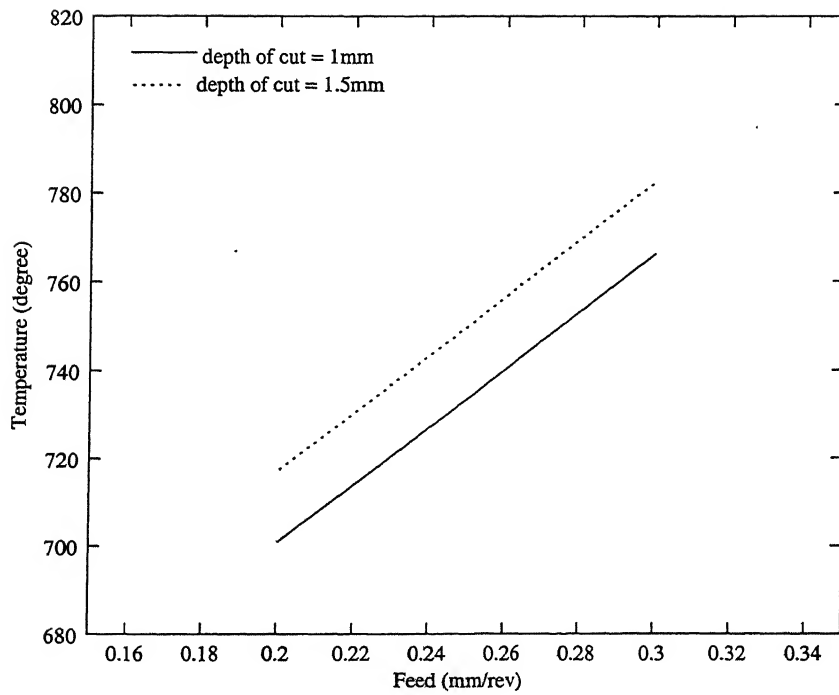


Figure 4.23 Variation of temperature with feed at 200 RPM

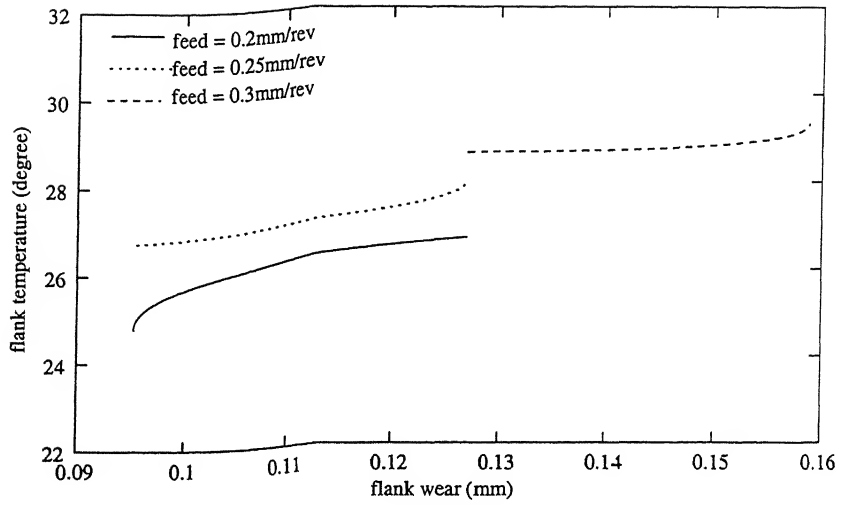


Figure 4.24 Variation of flank wear with flank temperature at 125 RPM

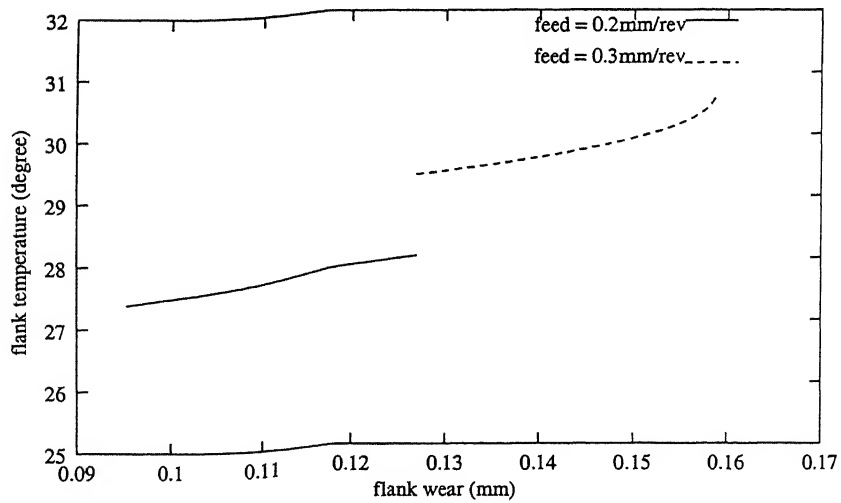


Figure 4.25 Variation of flank wear with flank temperature at 160 RPM

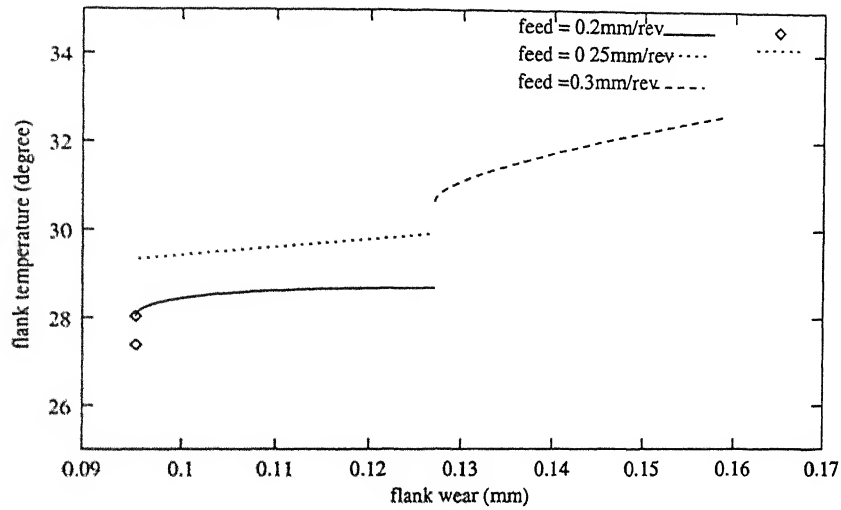


Figure 4.26 Variation of flank wear with flank temperature at 200 RPM

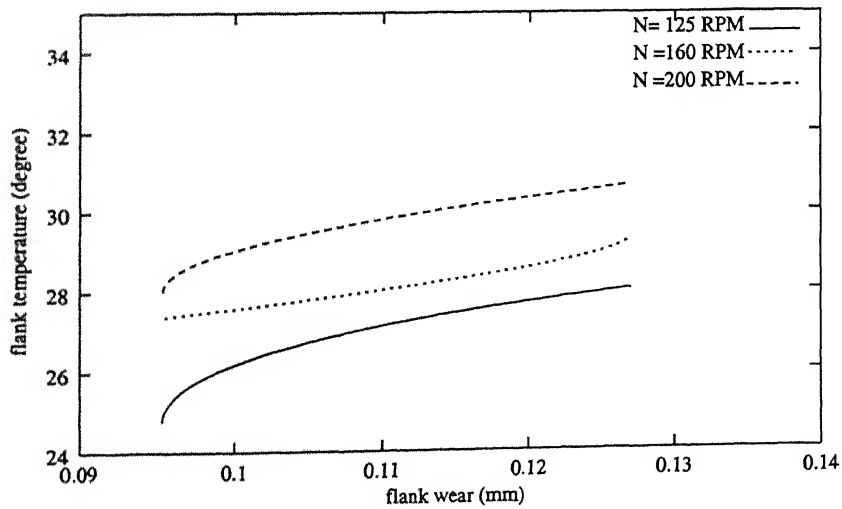


Figure 4.27 Variation of flank wear with flank temperature at 1mm depth of cut

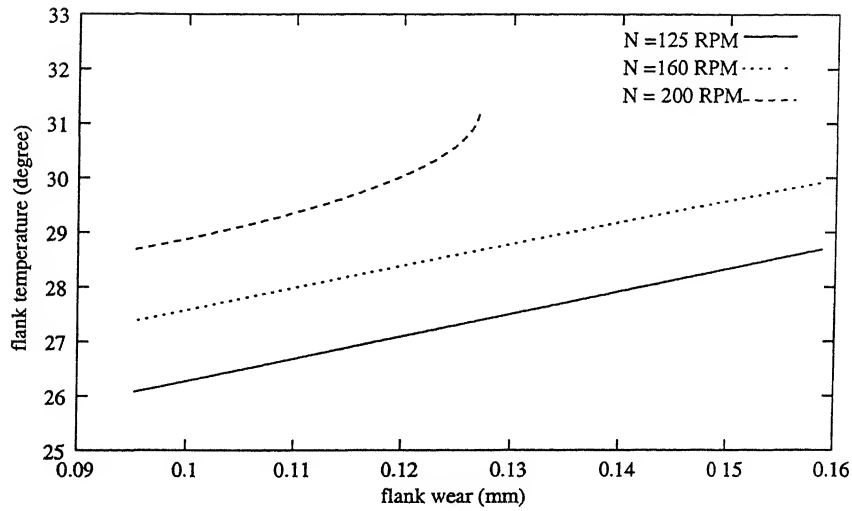


Figure 4.28 Variation of flank wear with flank temperature at 1.5mm depth of cut

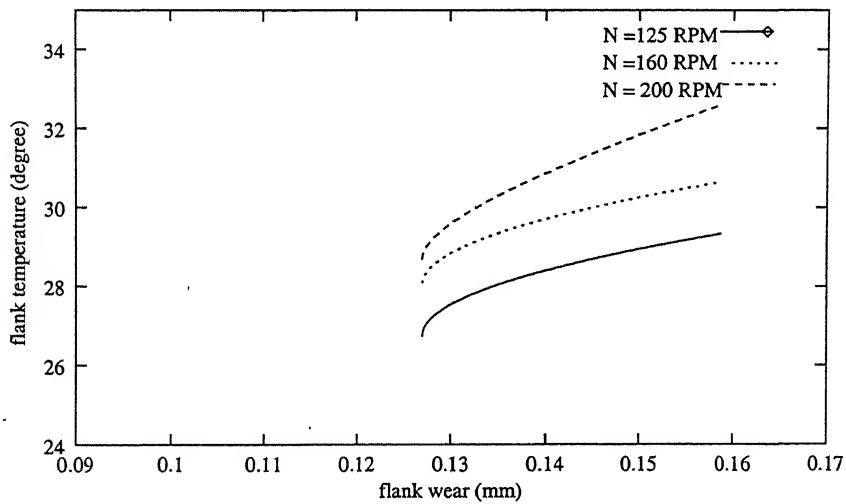


Figure 4.29 Variation of flank wear with flank temperature at 2.0mm depth of cut

Chapter 5

5.1 Conclusions:

The present work involved the measurement of temperature by the work tool thermocouple and relating it to the flank wear, which occurs. Factorial design was used in deciding the cutting parameters. The tests were conducted with HSS and WC tool bits. Temperature is one of the most important as well as a sensitive parameter, which governs the tool life. The effect of the flank temperature on the flank wear has been studied in the present work. The experimental results are compared with the theoretical results as obtained from the regression equation.

In this work, the assumption has been made that 0.04 of the total heat generated during the machining process is generated at the flank face of the tool. This assumption has been validated from the results obtained. If we compare the wear phenomena in HSS and WC tools we find that the effect of temperature on wear is more in case of the former than the latter. This is due to the material composition, which imparts different wear properties to the two materials. The 3^3 factorial design used in the present work is ideal because any other design would increase the number of experiments and the related calculations.

5.2 Scope for future work:

- a) The speed, feed and depth of cut range can be increased in case of the WC tool experiments
- b) It has been found that the A.C component of the thermoelectric signal is unaffected by the feed variations. Using an electronic filter the experiments can be performed.
- c) A variation of the 3^3 factorial design can be used in the experiments.

REFERENCES

- 1) R.L.Kegg, On line Machine and Process Diagnosis, *Annals of CIRP*, 32, 469- 473 (1984).
- 2) N.H.Cook, Tool Wear sensors, *Wear* 62, pp 49-57 (1980)
- 3) G.F. Michelliti, A De Fillippi and R.Ippolito, Tool wear and cutting forces in Steel Turning, *Annals of CIRP*, XVI, 353-360, (1968)
- 4) I.Inasaki and S.Yonetsu, In process detection of cutting tool damage by acoustic emission measurements, *Proceedings of 22nd International Machine Tool Design And Research Conference*, pp 261-268 (1981)
- 5) G.F.Michellitti, Tool Wear monitoring Through Acoustic Emission, *Annals of CIRP*, 32, 99-102, (1989)
- 6) N.H. Abu-Zahra And Taysir .H.Nayfeh, Calibrated Method for Ultrasonic On – Line Monitoring of gradual wear during turning operations, *International Journal of Machine Tools and Manufacture* Vol 37,pp,1475-1484, (1997)
- 7) D.Spirgeon and R.A.C. Slater, In process identification of surface roughness using a fibre-optics transducer, *Proceedings of 15th International Machine Tool Design and Research Conference* pp,339-347, (1974)
- 8) D.A.Stephenson, Tool-Work Thermocouple Temperature Measurements, Theory And Implementation Issues, *Transactions of ASME, Journal of Engineering for Industry*, Volume-115, pp, 432-437, (1993)
- 9) G.Barrow, A review of experimental and theoretical techniques for assessing cutting temperatures, *Annals of CIRP*, 22, 203-211 (1973)
- 10) A.A.Zakaria and J.I.Gomayel, On the reliability of the cutting temperature for monitoring tool wear, *International Journal of Machine Tool Design And Research* Vol.15, pp, 195-208, (1975)
- 11) P.Mathew,Use of Predicted Cutting Temperatures in Determining Tool Performance, *International Journal of Machine Tools And Manufacture*,Vol.29, No.4, pp 481-497, (1989)

- 12) M.P.Groover, R.J.Karpovich and E.K.Levy, A study of the relationship between remote thermocouple temperatures and tool wear in machining, *International Journal of Production Research*, Volume 25,No.2, pp 129-141,(1977)
- 13) D.R.Olberts, A study of the effects of Tool Flank Wear on Tool chip interface temperature, *Transactions of the ASME, Journal of Engineering for Industry*, pp152-158, May, 1959
- 14) E..K.Levy, C.L.Tsai,M.P. Groover, Analytical Investigation of the effect of Tool Wear on the temperature variations in a metal cutting tool, *Transactions of ASME, Journal of Engineering for Industry*,pp251-257,February, 1976
- 15) E.Lenz,Z.Katz and A.Ber, Investigation of the Flank Wear of Cemented Carbide tools, *Transactions of ASME, Journal of Engineering for Industry*,pp:246-250,1976
- 16) A.J.Wilkinson, Constriction-resistance applied to wear measurement of metal – cutting tools, *Proceeding of IEEE*, Vol.118, No.2, Feb 1971 pp: 381-386.
- 17) C.E.Leshock and Y.C.Shin, Investigation of Cutting temperature in Turning by a Tool work thermocouple technique, *Transactions of the ASME, Journal of Engineering for Industry*, Vol 119,November 1997, pp: 502-508.
- 18) On-line estimation of Tool-chip Interface Temperature for a Turning Operation,J.G.Chow and P.K. Wright, *Transactions of the ASME, Journal of Engineering for Industry*,Vol.110,February 1988,pp:56-64
- 19) Takeyama.H and Murata.R, Basic Investigation of Tool Wear, *Transactions of the ASME,Journal of Engineering for Industry*,Vol.85,February1963,pp.33.
- 20) E.F.Smart and E.M.Trent,Temperature distribution in tools used for cutting Iron,Titanium and Nickel, *International Journal of Production Research*,1975,Vol.13,No.3,pp:265-290.
- 21) Herchang Aay and Wen-Jei Yang, Heat Transfer and Life of metal Cutting tools used in turning, *International Journal of Heat and Mass Transfer*, Vol.41, No.3, pp: 613-623, 1998.
- 22) S.M.Wu and R.N.Meyer, Cutting Tool Temperature Predicting equation by Response Surface Methodology, *Transactions of the ASME, Journal of Engineering for Industry*, May1964,pp;150-156.

- 23) P.K.Venuvinod, W.S.Lau and C.Rubenstein, The role of Discrete Contact at the Flank Wear land in determining Cutting Tool Temperature in Orthogonal Cutting, *International Journal of Machine Tool Design and Research*, Vol23, No.4, pp:245-261, 1983.
- 24) P.M.Braiden, The Calibration of Tool-Work thermocouples, *Proceedings of 8th International Machine Tool Design and Research Conference*, 1967, pp: 653-666.
- 25) G.Boothroyd, J.M.Eagle and A.W.J.Chisholm, Effect of Tool Flank Wear on the Temperatures generated during Metal Cutting, *Proceedings of the 8th International Machine Tool Design and Research Conference*, 1967, pp: 667-680.
- 26) S.M.Wu, Tool Life Testing by Response Surface Methodology, *Transactions of The ASME, Journal of Engineering for Industry*, May 1964, pp: 105-110.
- 26a) S.M.Wu, Tool Life Testing by Response Surface Methodology, *Transactions of the ASME, Journal of Engineering for Industry*, May 1964, pp: 111-116.
- 27) Gerry Byrne, Thermoelectric Signal characteristics and Average Interfacial Temperatures in the machining of metals under geometrically defined conditions, *International Journal of Machine Tools and Manufacture*, Vol 27, No.2, pp:215-224, 1987.
- 28) P.W. Wallace, G. Boothroyd, Tool forces and tool – chip friction in orthogonal Machining, *International Journal of Mechanical Sciences*, 1964, 74-87.
- 29) T.H. Chu, J. Wallbank, Determination of the temperature of a machined Surface, *Journal of Manufacturing Science and Engineering*, May 1998, Vol 120, pp:259-263.
- 30) Tay, A.A. O, 1993, A Review of the Methods of calculating Machining Temperatures, *Journal of Material Processing Technology*, Vol36, pp 225-257.
- 31) A .Donavan and W.Scott, On line Monitoring of Cutting Tool Wear Through Tribo Emf Analysis, *International Journal of Machine Tools and Manufacture*, Vol35, No.11, pp 1523-1535, 1995.
- 32) A. Bhattacharya, Metal Cutting, Theory and Practice, Central Publishers, Calcutta.

- 23) P.K.Venuvinod, W.S.Lau and C.Rubenstein, The role of Discrete Contact at the Flank Wear land in determining Cutting Tool Temperature in Orthogonal Cutting, *International Journal of Machine Tool Design and Research*, Vol23, No.4, pp:245-261, 1983.
- 24) P.M.Braiden, The Calibration of Tool-Work thermocouples, *Proceedings of 8th International Machine Tool Design and Research Conference*, 1967, pp: 653-666.
- 25) G.Boothroyd, J.M.Eagle and A.W.J.Chisholm, Effect of Tool Flank Wear on the Temperatures generated during Metal Cutting, *Proceedings of the 8th International Machine Tool Design and Research Conference*, 1967, pp: 667-680.
- 26) S.M.Wu, Tool Life Testing by Response Surface Methodology, *Transactions of The ASME, Journal of Engineering for Industry*, May 1964, pp: 105-110.
- 26a) S.M. Wu, Tool Life Testing by Response Surface Methodology, *Transactions of the ASME, Journal of Engineering for Industry*, May 1964, pp:111-116.
- 27) Gerry Byrne, Thermoelectric Signal characteristics and Average Interfacial Temperatures in the machining of metals under geometrically defined conditions, *International Journal of Machine Tools and Manufacture*, Vol 27, No.2, pp:215-224, 1987.
- 28) P.W. Wallace , G. Boothroyd, Tool forces and tool – chip friction in orthogonal Machining, *International Journal of Mechanical Sciences*, 1964, 74-87.
- 29) T.H. Chu , J. Wallbank, Determination of the temperature of a machined Surface, *Journal of Manufacturing Science and Engineering*, May1998, Vol 120, pp:259-263.
- 30) Tay, A.A. O, 1993, A Review of the Methods of calculating Machining Temperatures, *Journal of Material Processing Technology*, Vol36, pp 225-257.
- 31) A .Donavan and W.Scott, On line Monitoring of Cutting Tool Wear Through Tribo Emf Analysis, *International Journal of Machine Tools and Manufacture*, Vol35, No.11, pp 1523-1535, 1995.
- 32) A. Bhattacharya, Metal Cutting, Theory and Practice, Central Publishers, Calcutta.

- 33) Archard, J.F. Contact and Rubbing of Flat Surfaces, *Journal of Applied Physics*, Vol.24, 1953.
- 34) Bhattacharya A , Ghosh .A and Ham, Inyong, Analysis of Tool Wear –Part 2. Application of Flank Wear Models, *Transactions of the ASME*, Paper No.69-WA/Prod.8.
- 35) V.C. Venkatesh, H.Chandrasekaran, Experimental Techniques in Metal Cutting. Prentice Hall of India, New Delhi, 1987.
- 36) D.C. Montgomery, Design and Analysis of Experiments, John Wiley and Sons.
- 37) B.L.Juneja and G.S. Sekhon, Fundamentals of Metal Cutting and Machine tools, Wiley Eastern Limited.

A. 141974



A141974